Archives of Biochemistry and Biophysics 754 (2024) 109932

Contents lists available at ScienceDirect

Archives of Biochemistry and Biophysics

journal homepage: www.elsevier.com/locate/yabbi

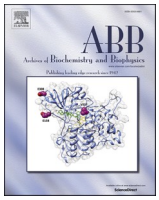

The catalytic action of human D-lactate dehydrogenase is severely inhibited by oxalate and is impaired by mutations triggering D-lactate acidosis

Alessandra Stefan [a,b], Alberto Mucchi [c], Alejandro Hochkoeppler [a,b,*]

[a] Department of Pharmacy and Biotechnology, University of Bologna, Viale Risorgimento 4, 40136, Bologna, Italy
[b] CSGI, University of Florence, Via della Lastruccia 3, 50019, Sesto Fiorentino, FI, Italy
[c] Department of Industrial Chemistry "Toso Montanari", Viale Risorgimento 4, 40136, Bologna, Italy

ARTICLE INFO

Keywords:
Human D-lactate dehydrogenase
Isoform 1
Isoform 2
Oxalate
T412 M variant
W323C variant

ABSTRACT

D-lactate dehydrogenases are known to be expressed by prokaryotes and by eukaryotic invertebrates, and over the years the functional and structural features of some bacterial representatives of this enzyme ensemble have been investigated quite in detail. Remarkably, a human gene coding for a putative D-lactate dehydrogenase (DLDH) was identified and characterized, disclosing the occurrence of alternative splicing of its primary transcript. This translates into the expression of two human DLDH (hDLDH) isoforms, the molecular mass of which is expected to differ by 2.7 kDa. However, no information on these two hDLDH isoforms is available at the protein level. Here we report on the catalytic action of these enzymes, along with a first analysis of their structural features. In particular, we show that hDLDH is strictly stereospecific, with the larger isoform (hDLDH-1) featuring higher activity at the expense of D-lactate when compared to its smaller counterpart (hDLDH-2). Furthermore, we found that hDLDH is strongly inhibited by oxalate, as indicated by a K_i equal to 1.2 μM for this dicarboxylic acid. Structurally speaking, hDLDH-1 and hDLDH-2 were determined, by means of gel filtration and dynamic light scattering experiments, to be a hexamer and a tetramer, respectively. Moreover, in agreement with previous studies performed with human mitochondria, we identified FAD as the cofactor of hDLDH, and we report here a model of FAD binding by the human D-lactate dehydrogenase. Interestingly, the mutations W323C and T412 M negatively affect the activity of hDLDH, most likely by impairing the enzyme electron-acceptor site.

1. Introduction

Lactate is generated by prokaryotic and eukaryotic cells through the action of stereospecific enzymes, exclusively yielding the L or the D enantiomer of this monocarboxylic acid [1]. The presence of L- and D-lactate dehydrogenases in the same organism was first shown for the bacterium *Lactobacillus plantarum*, with the concomitant presence of both enzymes recognized as responsible for the racemization of lactic acid [2–4]. At present, the repertoire of bacterial L-lactate dehydrogenases (LLDHs) contains NADH-dependent or –independent representatives [5], featuring a quaternary structure composed of two or four identical subunits [5,6]. Furthermore, prokaryotic LLDHs are known to exert their catalytic action according to Michaelis-Menten [5] or to cooperative kinetics [7], which is eventually modulated by homotropic or heterotropic effectors (e.g. by pyruvate and fructose-1, 6-bisphosphate, respectively). Bacterial D-lactate dehydrogenases (DLDHs) do also feature NADH-dependent or –independent activity, and they share with LLDHs a homodimeric [8–10] or homotetrameric assembly [11]. Moreover, similarly to LLDHs, D-lactate dehydrogenases isolated from bacterial sources obey Michaelis-Menten [12] or sigmoidal kinetics [13].

LLDHs were early detected in vertebrates, and two major subunits were identified, i.e. LDH-A and LDH-B, whose corresponding homotetramers are known as the muscle (M, LDH-5) and the heart (H, LDH-1) enzyme, respectively [14–16]. The H isoform is predominant in aerobic tissues, and its action is supposed to be mainly committed to the oxidation of lactate. Conversely, the M form is abundant in tissues exposed to transient hypoxia, e.g. in white muscle fibers, where it is engaged in the reduction of pyruvate. Curiously enough, over quite a number of years the expression of DLDHs was considered restricted to eukaryotic invertebrates [17]. However, the identification of genes coding for DLDHs in vertebrates suggested that both stereospecific lactate dehydrogenases can occur in these organisms [18]. Notably, vertebrate DLDHs belong to the VAO/PCMH (vanillyl alcohol

* Corresponding author. Department of Pharmacy and Biotechnology, University of Bologna, Viale Risorgimento 4, 40136, Bologna, Italy.
E-mail address: a.hochkoeppler@unibo.it (A. Hochkoeppler).

https://doi.org/10.1016/j.abb.2024.109932
Received 3 November 2023; Received in revised form 29 January 2024; Accepted 16 February 2024
Available online 17 February 2024

oxidase/*p*-cresol methylhydroxylase) flavoprotein family, whose members contain FAD or FMN as the redox cofactor [19,20], acting therefore as NADH-independent enzymes. In particular, vertebrate DLDHs are representatives of the α-hydroxy acid dehydrogenases subgroup of the VAO/PCMH flavoprotein family. It should also be noted that NADH-independent DLDHs are usually engaged in the oxidation of D-lactate, by this means taking part to the generation of pyruvate committed to the energetic metabolism. This implies, in turn, that DLDHs catalyse a thermodynamically-unfavourable reaction [21], the progression of which demands a prompt coupling of pyruvate synthesis and oxidative phosphorylation. Interestingly, quite a number of years ago the presence of D-2-hydroxy acid dehydrogenase activity in different organs of various vertebrates was assayed using D-lactate and 2, 6-dichlorophenolindophenol as electron acceptor [22]. In particular, high levels of DLDH activity were detected in kidneys of rabbit, ferret, and pigeon, as well as in rat liver [22].

In humans, three homotetrameric NADH-dependent LLDH isoforms are known: i) LLDH-5, to which the majority of structural and functional studies have been devoted [23,24]; ii) LLDH-1, featuring a high degree of structural similarity to LLDH-5 [25]; iii) LLDH-X, containing LDH-C subunits, and which is considered a testis-specific isoform [26,27]. In addition to these enzymes, a human gene coding for a putative DLDH has been identified [18], and an alternative splicing of the corresponding transcript is retained responsible for the translation of two isoforms whose molecular mass would differ by 2.7 kDa [18]. At present, no evidence at the protein level has been provided for these human DLDH isoforms.

Physiologically speaking, when cells are exposed to conditions limiting oxidative phosphorylation their energetic metabolism shifts to the generation of lactate. Accordingly, tissues subjected to fatigue and facing transient hypoxia feature a sixteen-fold increase of the lactate/pyruvate ratio when compared to resting counterparts [28]. However, it was demonstrated that lactate is produced in fully aerobic tissues [29,30], and it was therefore proposed that lactate always represents the end product of glycolysis [31]. According to this view, the cytosolic lactate generated under aerobic conditions shuttles to the mitochondrial intermembrane space, where it is converted to pyruvate, which is finally committed to the Krebs cycle [31]. Notably, when the generation of lactate dominates the energetic metabolism, the intracellular pH undergoes a substantial decrease. However, it should be noted that the reduction of pyruvate exerted by LDH at the expense of $NADH + H^+$ does not induce acidification *per se*, being instead a proton-consuming reaction. Actually, lactic acidosis stems from a net release of H^+ from ATP hydrolysis under hypoxic or anoxic conditions [32]. Considering the relevance of L-lactate in cytosolic acidosis and in the energetic metabolism of cancer cells, substantial work is devoted to improve our understanding about how the action of LLDHs affects the fate of cells. In addition, the search for effective and selective inhibitors of human LLDHs is strongly pursued with the aim to provide innovative therapeutic agents against cancer [33,34].

Contrary to the large interest raised by human LLDHs, the information available on their D-counterparts is rather poor. It is important to mention that D-lactate can be generated at the expense of methylglyoxal (MG), a toxic metabolite mainly produced from dihydroxyacetone phosphate and glyceraldehyde-3-phosphate [35–37]. The detoxification of methylglyoxal is primed by its conjugation with glutathione, and the resulting hemithioacetal is then converted by glyoxalase I to S-lactoylglutathione [38]. Finally, glyoxalase II catalyzes the release of D-lactate and glutathione from S-lactoylglutathione [38]. Remarkably, effective experiments demonstrated that human glyoxalase III detoxifies methylglyoxal yielding L-lactate, whereas the homologous enzyme from *Arabidopsis thaliana* converts MG into D-lactate [39]. Accordingly, D-lactate is generated in human cells by glyoxalase I/II only, and this detoxification route proceeds further with the oxidation of D-lactate. This occurs in mitochondria, which were shown to be competent in oxidizing D-lactate to pyruvate, yielding by this means a useful energy source [40]. Remarkably, it was also observed that the activity of DLDH is higher in human cancer cells than in their normal mates [40]. Further, different diseases are phenotypically associated with high (mM) levels of D-lactate in plasma and urine [41–44]; however, it should be mentioned that the clinical relevance of this phenotype (denoted as D-lactate acidosis) is actually questioned [45]. Nevertheless, it was recently demonstrated with very elegant experiments that human DLDH is responsible for the oxidation of D-lactate *in vivo*. In particular, two site-specific variants (W374C and T463 M) of human DLDH were detected in patients suffering of D-lactate acidosis [46]. When these variants were expressed in zebrafish bearing a knockout allele of the DLDH-coding locus, the concentration of D-lactate did significantly increase when compared to the level detected in wild-type animals [46]. It is also of importance to note that the expression of wild-type human DLDH in the knocked-out zebrafish was shown to suffice to the containment of D-lactate concentration within physiological values [46]. Remarkably, these experiments do unambiguously demonstrate that human DLDH is competent in oxidizing D-lactate *in vivo*, therefore aiding in the containment of D-lactate acidosis.

Considering the potential relevance of D-lactate under different pathological conditions, we thought it of interest to investigate both isoforms of human DLDH at the protein level. Accordingly, we report here on kinetic and structural features of these two enzymes, along with a detailed analysis of the effects triggered by the mutations W374C and T463 M on the catalytic action of human D-lactate dehydrogenase.

2. Materials and Methods

2.1. Materials

All reagents were obtained by Merck-Millipore (Burlington, MA, USA). Sodium D-lactate (≥99%) was used without further purification.

2.2. Protein overexpression and purification

The UniProt accession ID for the human D-lactate dehydrogenase (DLDH) is Q86WU2, and according to the information associated with this entry (https://www.uniprot.org/uniprotkb/Q86WU2) the amino acids 1–52 of the corresponding primary structure represent the signal peptide responsible for mitochondrial targeting of DLDH. Therefore, we decided to overexpress in *Escherichia coli* the corresponding full-length mature human DLDH, i.e. the protein containing residues 53–507 of the Q86WU2 entry, denoted here as hDLDH-1 (Supplementary Figs S1A and S1B). It should be mentioned that to counteract the occurrence of intermolecular disulfide bonds, the C176*S* mutation was introduced in hDLDH-1 (C227*S* using the precursor coordinates), with this single-site variant representing the target to be overexpressed in *E. coli*. Considering the evidence supporting an alternative splicing of the transcript coding for hDLDH [18], we also overexpressed the resulting isoform (denoted as hDLDH-2), lacking residues 211–233 of the precursor sequence (amino acids 160–182 of hDLDH1, Supplementary Figs S1A and S1C).

To overexpress the isoforms of hDLDH, a couple of genes, optimized for *E. coli* codon usage, was synthesized (GenScript, Leiden, NL). Both genes (Supplementary Fig. S1) were cloned into the pET9a vector, using the *Nde*I and *BamH*I sites, and the constructs accordingly obtained were used to transform *E. coli* BL21(DE3). Transformants were selected on LB-kanamycin (40 μg/mL) Petri dishes, and subsequently purified on LB-kan plates. Single colonies were then picked to inoculate LB-kan liquid medium, and grown for 15 h at 37 °C under shaking conditions (180 rpm). The pre-cultures accordingly obtained were diluted (1:500) into fresh LB-kan medium and grown at 30 °C for 9 h. Then, 1 mM isopropyl-β-D-thiogalactopyranoside (IPTG) was added, and the induced cultures were incubated at 30 °C for 15 h. Induced cells (200 mL) were harvested by centrifugation (4500×*g*, 20 min, 4 °C), and the pellets were resuspended in 20 mL of 50 mM Tris-HCl, 50 mM NaCl, pH 8. Total proteins

were extracted by sonication (Misonix-3000 sonifier, output level of 18 W for 15 s, followed by a 15 s cooling interval, for 4 cycles).

Both hDLDH isoforms were recovered from the insoluble fraction of the protein extract as we previously described [47,48]. In particular, the total protein extract was centrifuged at 13,000×*g* (30 min, 4 °C), and the pellet containing the inclusion bodies was resuspended in 10 mM Tris-HCl, 1 % (w/v) N-lauroylsarcosine, pH 7.5. The suspension was incubated at 4 °C for 15 h under mild shaking, and then centrifuged at 13,000×*g* (30 min, 4 °C). The supernatant accordingly obtained (ca. 20 mL) was supplemented with 1.875 g of Amberlite XAD-4, and the mixture was mildly stirred for 3 h, at room temperature. Finally, the resin was decanted and discarded, and the resulting solution was centrifuged at 13,000×*g* (30 min, 4 °C). After discarding the pellet, the protein solution was supplemented with 2.5 mM DTT, concentrated to approximately 2 mL and loaded onto a Superdex 200 column (1.6 × 60 cm), previously equilibrated with 10 mM Tris-HCl, pH 7.5. Elution was performed at 0.6 mL/min, and fractions of 0.9 mL were collected. The column was calibrated with HMW and LMW Gel Filtration Calibration kits (Cytiva, Uppsala, Sweden), using dextran blue, ferritin, catalase, aldolase, albumin, ovalbumin, chymotrypsinogen A, and RNase A. The best eluted fractions, according to SDS-PAGE analysis, were pooled, concentrated, supplemented with 0.4 M sucrose (final concentration), and stored at −20 °C until used.

Protein concentration was determined according to Bradford [49].

2.3. Mutagenesis

Site specific mutagenesis of the synthetic gene coding for hDLDH-1 was performed by GenScript (Leiden, NL). In particular, the W323C mutant was obtained replacing the TGG codon with TGC, and the T412 M variant was constructed substituting the ACC codon with ATG. Both genes subjected to mutagenesis were sequenced to confirm the identity of the mutations. No site-specific substitutions in addition to those desired were detected by sequencing.

2.4. Activity assays

The catalytic activity of hDLDH at the expense of D-lactate was spectrophotometrically assayed. Assay mixtures contained 15 mM D-lactate, 50 μM 2,6-dichlorophenolindophenol (DCPIP) in 50 mM Tris-HCl, 5 mM EDTA, 0.1 % (w/v) Triton X-100, pH 7.5. The reaction was observed at 600 nm using a Cary 300 Bio spectrophotometer, and the extinction coefficient (ε) of DCPIP was considered equal to 21 $mM^{-1}cm^{-1}$ [50]. Alternatively, the oxidation kinetics of D-lactate was determined at 275 nm in the presence of decylubiquinone in 50 mM Tris-HCl, 5 mM EDTA, pH 7.5. To this aim, a stock solution containing 100 mM decylubiquinone in DMSO (stored at −20 °C) was diluted 1:10 in ethanol immediately before the assays were performed. In addition, the competence of hDLDH in transferring electrons to horse heart cytochrome *c* was tested at 550 nm. The reduced-minus-oxidized $\Delta\varepsilon$ of cytochrome *c* was considered equal to 21.1 $mM^{-1}cm^{-1}$ [51].

2.5. Inhibition assays

The inhibition of hDLDH-1 by amino acids, oxalate, oxamate, or pyruvate was tested in 50 mM Tris-HCl, 5 mM EDTA (pH 7.5), in the

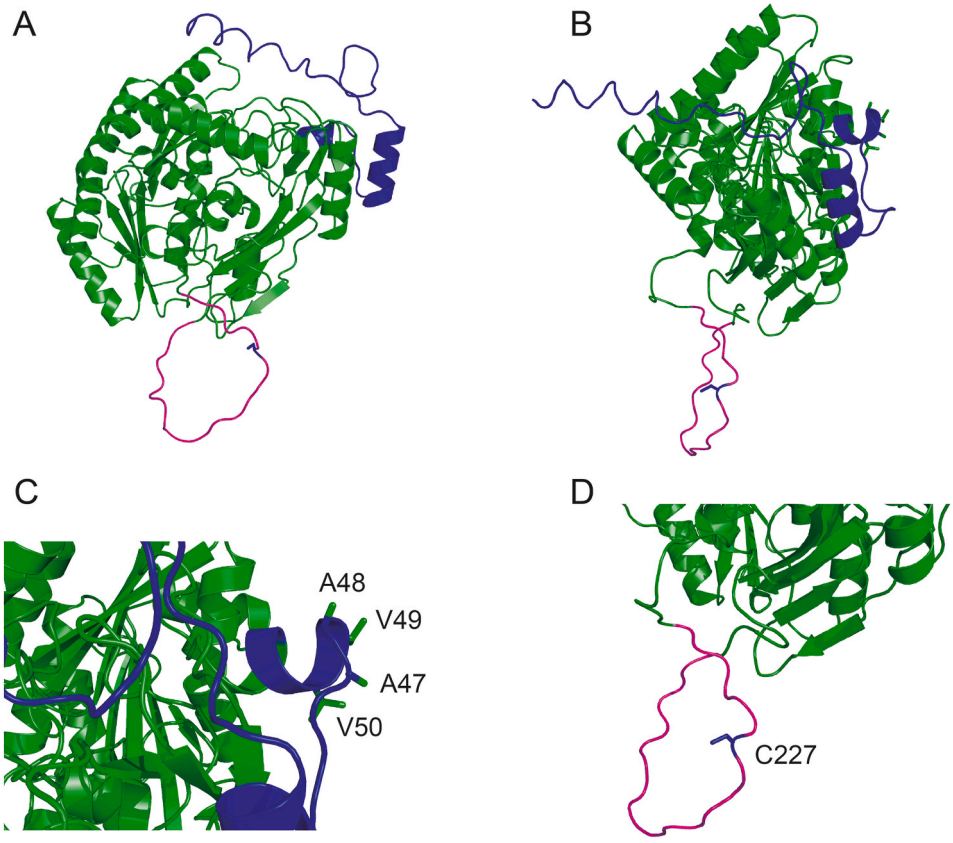

Fig. 1. Structural model of human D-lactate dehydrogenase (hDLDH).
(**A,B**) Model provided by AlphaFold of the tertiary structure of human D-lactate dehydrogenase (hDLDH). The signal peptide, consisting of residues 1–52, is reported in blue. The structural region pertaining to the mature enzyme is depicted in green and magenta. The transcript coding for hDLDH undergoes alternative splicing, generating two enzyme isoforms, which differ for the presence or the absence of an extended loop (reported in magenta) containing the amino acids 211–233 (159–181 in the mature protein). (**C**) Detail of the N-terminal region of hDLDH. The residues 47–50 are represented with sticks to show their exposure to the solvent. (**D**) Close view of the loop connecting residues 210–234 of hDLDH. Cysteine 227 is represented in blue.

presence of 1 μM enzyme, 15 mM D-lactate, and 50 μM DCPIP. The inhibition exerted by oxalate, oxamate, and pyruvate on the hDLDH-1 catalytic action was quantitatively inspected according to the equation [52]:

$$\frac{1}{v} = \frac{[S] + K_m}{V_{max}[S]} + \frac{K_m}{V_{max}[S]K_i}[I] \quad (1)$$

where K_i is the inhibition constant, and $[I]$ indicates the concentration of the inhibitor.

2.6. Dynamic light scattering

Dynamic light scattering experiments were performed with a Malvern Panalytical (Malvern, UK) Zetasizer Nano ZS system, using the fractions eluted from the Superdex 200 column and representing the maximum of the detected peaks (see above). All the measurements were recorded at 25 °C using solutions previously filtered with 0.2 μm filters. Scattering was evaluated at an angle of 173°. Each sample was subjected to three consecutive analyses, each consisting of the average of 12–15 determinations. Raw data were analyzed with the Zetasizer software (Malvern Panalyticals), release 7.11.

2.7. Circular dichroism

CD spectra were recorded over the 200–250 nm wavelength interval at a scan rate equal to 50 nm/min, using a Jasco J-810 spectropolarimeter and a 0.5 cm path-length cuvette. Protein samples were in PBS, and the bandwidth was set to 1 nm. Sixteen scans per sample were acquired and averaged.

2.8. Atomic emission spectroscopy

The iron concentration in liquid hDLDH samples was determined using an Agilent MP-AES 4210 Spectrometer. The emission intensities of standards and samples were determined at three different wavelengths, namely 371.993, 373.486, and 385.991 nm, respectively. Nitric acid (VWR Normatom, cod. 83872.270) and demineralized water (Millipore DirectQ, resistivity 18.2 MΩ • cm) were used to prepare all analytical standards and samples. A commercial iron standard (1 g/L, VWR Titrinorm, code 86677.260) was diluted to obtain solutions having the following concentrations of iron: 0.05, 0.10, 0.50, 1.00, and 2.00 mg/L. A blank standard was also prepared and used throughout. Nitric acid (0.94 %, m/v, final concentration) was added to all calibration standards.

Two samples, containing 61 and 32.5 μM hDLDH-1 and hDLDH-2, respectively, were diluted 1:5 by adding Millipore demineralized water and nitric acid to a final concentration of 0.94 % (m/v), and they were subsequently analyzed. Three blanks were also prepared and subjected to the same analytical procedure of the protein samples.

To determine the detection limit (LoD) and the quantification limit (LoQ), we calculated the concentration corresponding to the values obtained (at the three wavelengths) by adding to the mean of the blank standards 3.2 and 10 times, respectively, their standard deviation. The final parameters were obtained from the quadratic average of the three values, multiplied by 5 (the dilution factor).

2.9. Structural analyses of hDLDH

The analyses and representations of the tertiary structure of hDLDH and *Escherichia coli* DLDH were rendered with PyMol (release 2.5.2, [53]).

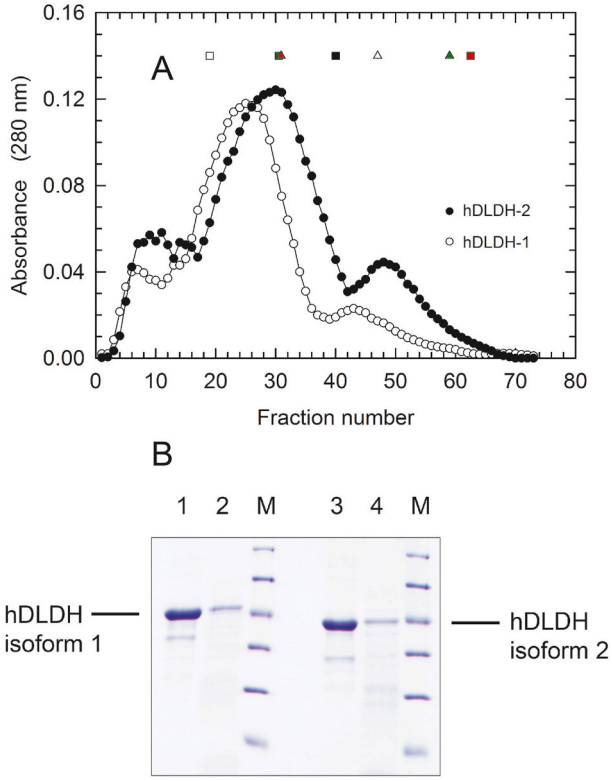

Fig. 2. Purification of hDLDH.
(**A**) Gel filtration chromatography of hDLDH-1 (white circles) and hDLDH-2 (black circles) isoform of human D-lactate dehydrogenase. Both isoforms were previously subjected to solubilization from inclusion bodies by means of sarkosyl and subsequently refolded using Amberlite XAD-4. The refolded enzymes were then loaded onto a Superdex 200 column, the calibration of which was performed with ferritin (440 kDa, white square), catalase (232 kDa, green square), aldolase (158 kDa, red triangle), albumin (67 kDa, black square), ovalbumin (43 kDa, white triangle), chymotrypsinogen A (25 kDa, green triangle), RNase A (13.7 kDa, red square). (**B**) SDS-PAGE of the purified isoforms of hDLDH. The best fractions of hexameric and monomeric hDLDH-1 eluted from the Superdex column were pooled, concentrated and loaded onto lanes 1 and 2, respectively. The pools of purified tetrameric and monomeric hDLDH-2 were loaded onto lanes 3 and 4, respectively. The molecular masses of the loaded markers (lanes M) are (top to bottom) 116, 66.2, 45, 35, 25, and 18.4 kDa, respectively.

3. Results

3.1. Overexpression and purification of human DLDH isoforms

To prime our analysis of the two isoforms of hDLDH [18], we inspected the structural model of the precursor enzyme provided by AlphaFold (Figs 1A and 1B, file PDB: AF-Q86WU2–F1-model_v4). Interestingly, this model reveals that the portion of the signal peptide distal from the N-terminus (see Methods and Figs 1B and 1C) contains 4 surface-exposed hydrophobic amino acids, i.e. A47, A48, V49, and V50, respectively (Fig. 1C). Therefore, we decided to construct two synthetic genes coding for the two isoforms of hDLDH, with both enzymes devoid of the amino acids 1–52 of the precursor protein. The structural model of hDLDH does also disclose that C227 (precursor coordinates, C176 of mature hDLDH isoform 1) is not engaged in any intramolecular disulfide bridge, being therefore able to take part in intermolecular S–S bonds (Figs 1A, 1B, and 1D). Accordingly, to avoid this possibility we introduced in the isoform 1 of hDLDH (hDLDH-1) the C176S mutation (the protein coordinates used hereafter are those referring to the mature hDLDH isoforms). It should also be noted that C176 is absent in hDLDH isoform 2 (hDLDH-2), which lacks the protein region containing this

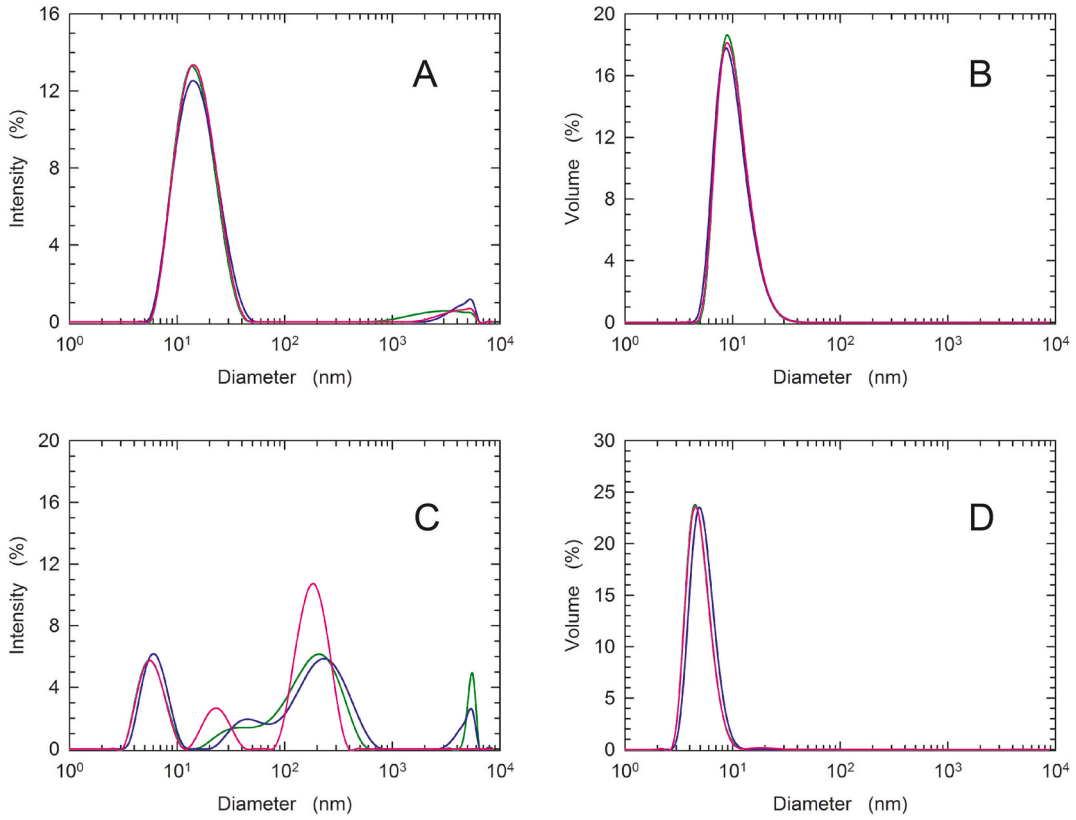

Fig. 3. Dynamic light scattering experiments performed with hDLDH-1.
(**A-D**) The output of three independent measurements (green, blue, and magenta lines) obtained with purified hexameric (**A,B**) and monomeric (**C,D**) hDLDH-1 is shown. The percentage of scattering intensity (**A,C**) by the detected particles is reported as a function of their diameter. The percentage volume (**B,D**) of the particles as a function of their diameter is also shown.

cysteine (Figs 1A and 1B).

To overexpress the two hDLDH isoforms, a couple of genes, optimized for the *Escherichia coli* codon usage, were synthesized (Supplementary Fig. S1) and cloned into the vector pET9a. The constructs accordingly obtained were used to transform *E. coli* BL21(DE3), and the overexpression of the target proteins was performed by means of standard techniques (see Methods). Notably, we obtained comparable expression yields, equal to ca. 400 mg/L, for hDLDH-1 and hDLDH-2. It should also be mentioned that both isoforms were recovered from the insoluble fraction of protein extracts isolated from cells induced to overexpression (Supplementary Fig. S2A). Further, to solubilize and refold the two isoforms of hDLDH we took advantage of our recently reported procedure which entails N-lauroylsarcosine (also denoted as sarkosyl) as the solubilizing agent, and Amberlite XAD-4 as a convenient tool to refold a target protein dissociated from inclusion bodies with the aid of sarkosyl (Supplementary Fig. S2B) [47,48].

Interestingly, when refolded hDLDH-1 was subjected to gel filtration chromatography two association states of this enzyme were detected, featuring molecular mass equal to 295 and 68 kDa, respectively (Fig. 2A). Considering an expected molecular mass of 49.2 kDa, these states correspond to hexameric and monomeric hDLDH isoform 1, respectively. It is also interesting to note that the amount of hexamer does largely prevail over that of the monomer (Figs 2A and 2B), with yields of purified protein equal to 230 and ca. 2 mg/L, respectively. When gel filtration chromatography was used to analyze hDLDH-2, the elution volume of the major observed peak translates into a molecular mass equal to 195 kDa (Fig. 2A). Taking into account that the expected molecular mass of hDLDH-2 is equal to 46.5 kDa, this corresponds to a tetrameric quaternary structure of the enzyme (Fig. 2A). In addition to this oligomeric state, we also detected monomeric hDLDH-2, the molecular mass of which was determined as equal to 44.7 kDa (Fig. 2A). Similarly to what we observed with hDLDH-1, the amount of monomeric hDLDH-2 recovered from the gel filtration column was much lower when compared to that of the tetramer (Figs 2A and 2B). In particular, we obtained yields equal to 265 and ca. 2 mg/L for the tetramer and for the monomer of hDLDH-2, respectively.

3.2. Dynamic light scattering experiments

To further inspect the oligomeric states of hDLDH, we performed dynamic light scattering (DLS) experiments. Remarkably, when hDLDH-1 was analyzed, an excellent agreement was observed between the molecular mass values estimated by means of gel filtration chromatography and DLS. We indeed determined by DLS an apparent molecular mass of hDLDH-1 equal to 296 kDa, with this value corresponding to an hexameric quaternary structure (Figs 3A and 3B). Moreover, it is important to note that this hDLDH-1 quaternary structure appears to be rather stable. Actually, when three successive DLS analyses of this isoform were carried out, no significant differences among the observed oligomeric states were observed (Fig. 3A), with molecular mass values of 296 ± 166, 296 ± 199, and 296 ± 176 kDa, respectively. On the contrary, when monomeric hDLDH-1 was subjected to three consecutive DLS analyses we detected substantial changes in the apparent dimension of this form (Figs 3C and 3D), with molecular mass values estimated as equal to 38 ± 26, 53 ± 26, and 38 ± 13 kDa. Accordingly, the analysis by DLS of the molecular mass of monomeric hDLDH-1 is affected by a conspicuous error, yielding a mean value of 43 ± 9 kDa. In addition, and surprisingly, different aggregates were observed to occur with monomeric hDLDH-1 (Fig. 3C), albeit they do not represent a major component of the sample volume (Fig. 3D). It is important to note here that the DLS analyses were carried out immediately after the elution of hexameric and monomeric hDLDH-1 from the gel filtration column.

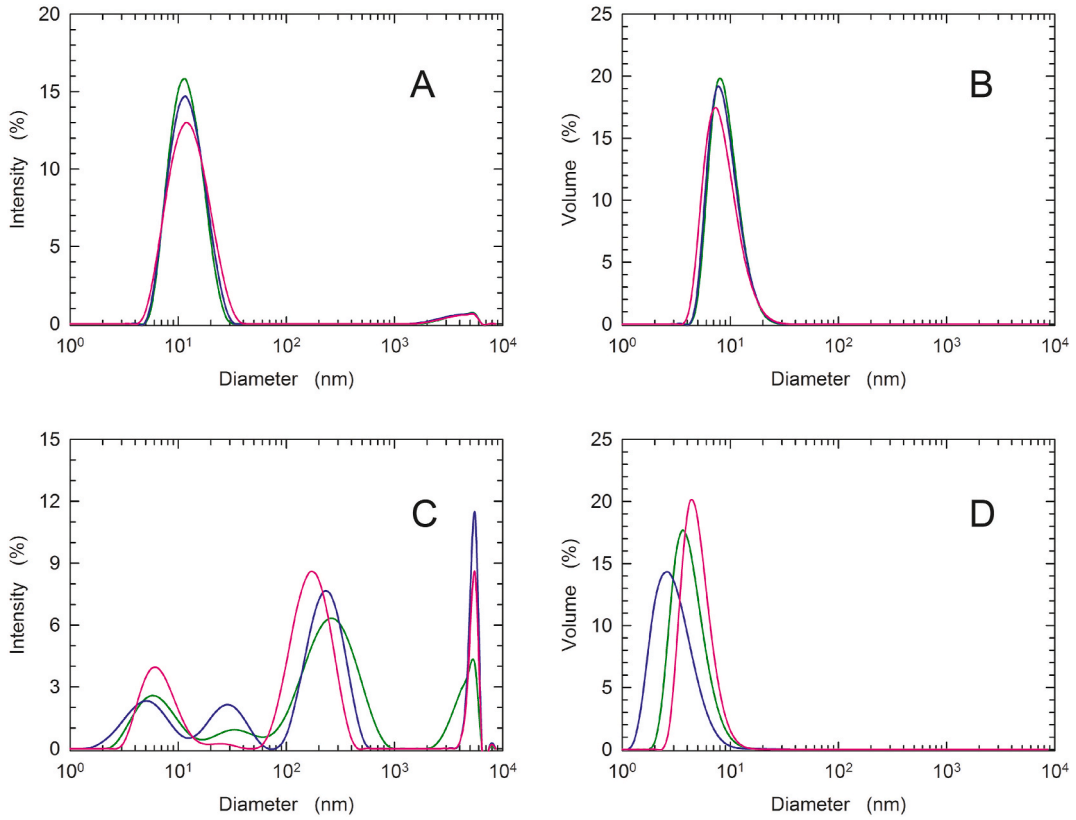

Fig. 4. Dynamic light scattering experiments performed with hDLDH-2.
(**A-D**) The output of three independent measurements (green, blue, and magenta lines) obtained with purified tetrameric (**A,B**) and monomeric (**C,D**) hDLDH-2 is shown. The percentage of scattering intensity (**A,C**) by the detected particles is reported as a function of their diameter. The percentage volume (**B,D**) of the particles as a function of their diameter is also shown.

Therefore, the various aggregates accompanying monomeric hDLDH-1 appear to be generated by a rapid association of monomers. Remarkably, this feature of monomeric hDLDH-1 is quite likely responsible for the lower yield that we obtained for this form when compared to that obtained for hexameric hDLDH-1.

Generally speaking, the molecular features of hDLDH-2 that we observed performing DLS experiments resemble those detected in the presence of hDLDH-1. When the oligomeric state of hDLDH-2 was analyzed by DLS, a molecular mass of 213 ± 7 kDa was determined (Figs 4A and 4B), in good agreement with the value evaluated by gel filtration chromatography, i.e. 195 kDa. Accordingly, and taking into account an expected molecular mass of 46.5 kDa, the DLS experiments indicate a tetrameric assembly for the oligomeric state of hDLDH-2. Further, the tetrameric hDLDH-2 quaternary structure proved to be stable, as suggested by three successive DLS analyses (Fig. 4A). On the contrary, monomeric hDLDH-2 was found to be unstable and prone to aggregation (Fig. 4C), with its molecular mass determined as equal to 38 ± 16, 27 ± 12, and 53 ± 24 kDa. These estimates correspond to a mean of 39 ± 13 kDa, which does not significantly differ from the mean value of the molecular mass determined for monomeric hDLDH-1. As previously mentioned for hDLDH-1, although the aggregated forms of monomeric hDLDH-2 do not represent an extensive part of the total enzyme volume (Fig. 4D) the unstable nature of the monomer is quite likely responsible for the low yield that we obtained for this enzyme.

3.3. Structural features of human DLDH isoforms

To further characterize both hDLDH isoforms, we analyzed their secondary structure by means of CD spectroscopy. In particular, when considering that monomeric hDLDH is prone to aggregation, we determined the far-UV CD spectrum of hexameric hDLDH-1 and tetrameric hDLDH-2 only. Overall, the two observed spectra are similar, with a minimum at 208 nm which is more pronounced in the spectrum of hDLDH-2 (Fig. 5A). To perform a quantitative analysis of these data, we used the K2D algorithm [54] via the DichroWeb server [55]. According to this analysis, hexameric hDLDH-1 features 30, 14, and 56 % of amino acids belonging to α-helices, β-strands, and coils, respectively (Fig. 5B). Interestingly, performing the same analysis using the CD spectrum of hDLDH-2 we obtained a secondary structure composed of 23, 22, and 54 % residues located in α-helices, β-strands, and coils, respectively (Fig. 5C). These data can be compared with those obtained analyzing the model of hDLDH tertiary structure generated by AlphaFold (Fig. 1). According to this model, the precursor of hDLDH contains 16 α-helices and 15 β-strands, and the loop exclusively present in hDLDH-1 is composed of 23 amino acids (Fig. 1). Furthermore, taking into account the portion of the AlphaFold model which refers to mature hDLDH, we estimated the relative abundance of amino acids into the different elements of secondary structure. By this means, hDLDH-1 was found to contain 38, 18, and 44 % of residues in α-helices, β-strands, and random coils, respectively. This evaluation is in reasonable agreement with the analysis performed using the CD spectrum of hDLDH-1, with the major difference pertaining the relative abundance of amino acids belonging to α-helices (30 vs. 38 %). This discrepancy is more pronounced when hDLDH-2 is considered: for this isoform the AlphaFold structural model does indeed suggest a secondary structure composed of 40, 20, and 40 % of amino acids being located in α-helices, β-strands, and random coils, respectively. Similarly to what observed with hDLDH-1, the major difference between these data and those obtained by CD spectroscopy resides in the relative abundance of α-helices.

Using mitochondria isolated from human prostate cells and performing activity assays detecting D-lactate oxidation, D-lactate dehydrogenase was shown to be associated with the matrix side of the inner

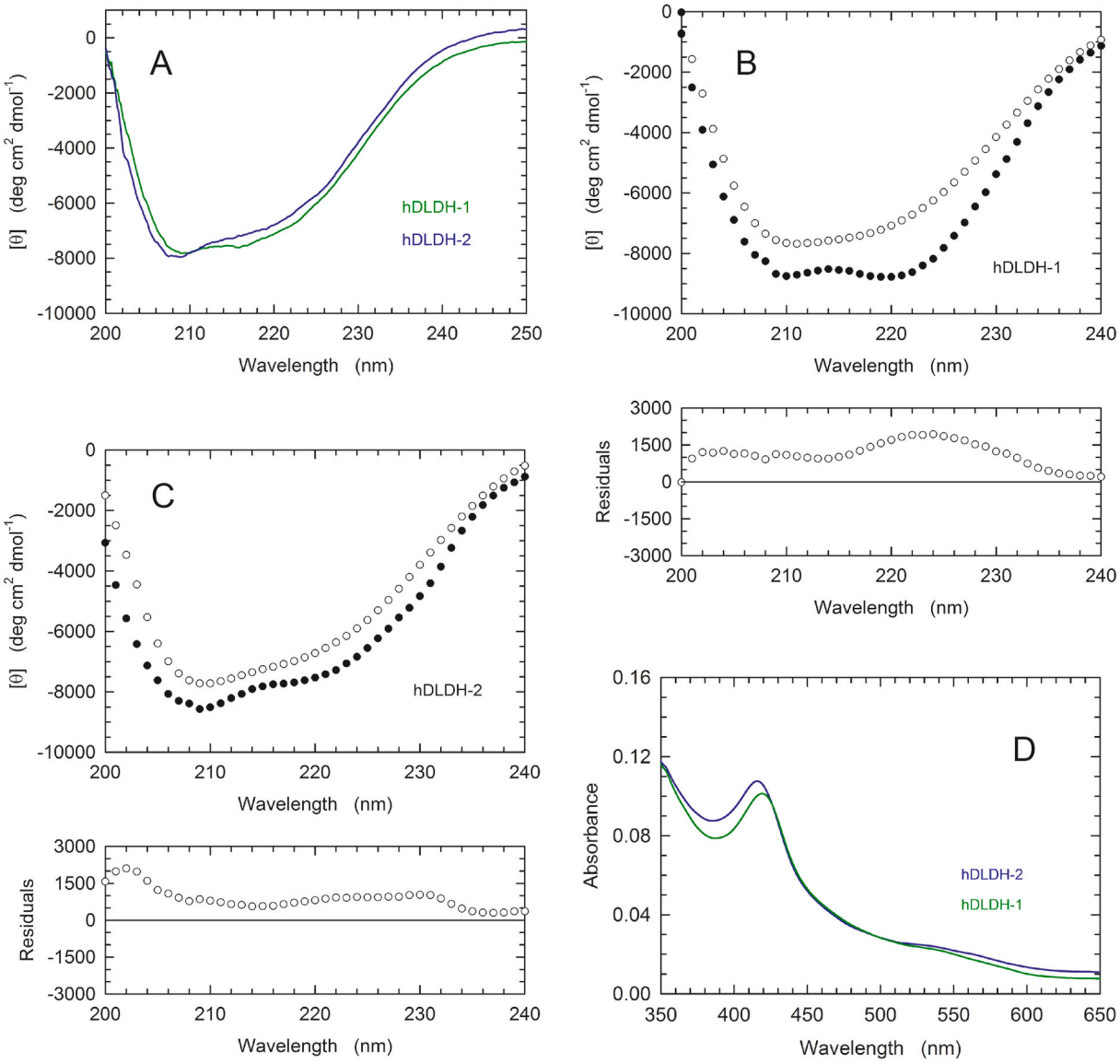

Fig. 5. Structural features of human D-lactate dehydrogenase.
(**A**) CD spectra of hDLDH-1 (green line) and hDLDH-2 (blue line) in PBS buffer, pH 7.5. (**B**) Observed (white circles) and predicted (black circles) CD spectrum of hDLDH-1. The residuals represent the observed minus expected difference values. (**C**) Observed (white circles) and predicted (black circles) CD spectrum of hDLDH-2. The residuals represent the observed minus expected difference values. (**D**) Absorption spectrum of 203 μM hDLDH-1 (green line) and 215 μM hDLDH-2 (blue line) in 10 mM Tris-HCl buffer, pH 7.5.

mitochondrial membrane [40]. Moreover, fluorimetric assays carried out with cell lysates revealed that human D-lactate dehydrogenase is a FAD-dependent enzyme [40]. To identify the cofactor associated to purified hDHLDH-1 and hDHLDH-2, we recorded the UV–Vis absorption spectra of both isoforms over the 350–650 nm wavelength interval. Surprisingly enough, when hDLDH-1 and hDLDH-2 were analyzed we did not detect an absorption spectrum diagnostic of FAD (Fig. 5D). Indeed, instead of the characteristic broad absorption band of FAD, featuring a maximum at 450 nm, the spectra of the hDLDH isoforms showed a single sharp band with maximal absorption shifted to shorter wavelengths (Fig. 5D). In particular, the two spectra resulted quite similar, with the main distinctive trait represented by a slight shift of the absorption maximum, located at 420 and 416 nm when the absorption bands of hDLDH1 and hDLDH2 are considered, respectively (Fig. 5D). To interpret the outcome of this spectroscopic analysis of the two hDLDH isoforms, we reasoned that their absorption bands could suggest the occurrence of a heme cofactor. However, when hDLDH-1 was exposed to oxidizing and subsequently to reducing conditions we did not detect significant Absorbance changes in the wavelength interval over which the presence of hemoproteins can be revealed (Supplementary Fig. S3). The presence in hDLDH of a FeS cluster was then considered. First, the spectrum of hDLDH-1 was recorded in the absence or in the presence of an excess of sodium dithionite (Fig. 6A). Interestingly, under reducing conditions we detected the unabridged bleaching of the enzyme absorption band centered at 420 nm (Figs 6A and 6B), with this observation resembling the difference spectra reported for quite a number of ferredoxins [56,57] and for the High Potential Iron Sulfur Protein (HiPIP) from *Chromatium* [57]. Therefore, we analyzed both hDLDH isoforms by microwave plasma atomic emission spectroscopy (MP-AES). In particular, immediately before the analysis we dialyzed hDLDH-1 and hDLDH-2 against ultrapure water, and we assayed the dehydrogenase activity of the dialyzed enzymes. Remarkably, performing these assays under standard conditions (15 mM D-lactate, 50 μM 2,6-dichlorophenol indophenol, 50 mM Tris-HCl, 5 mM EDTA, pH 7.5) no significant differences were observed between the activity levels detected using the buffered and the dialyzed enzyme stock solutions.

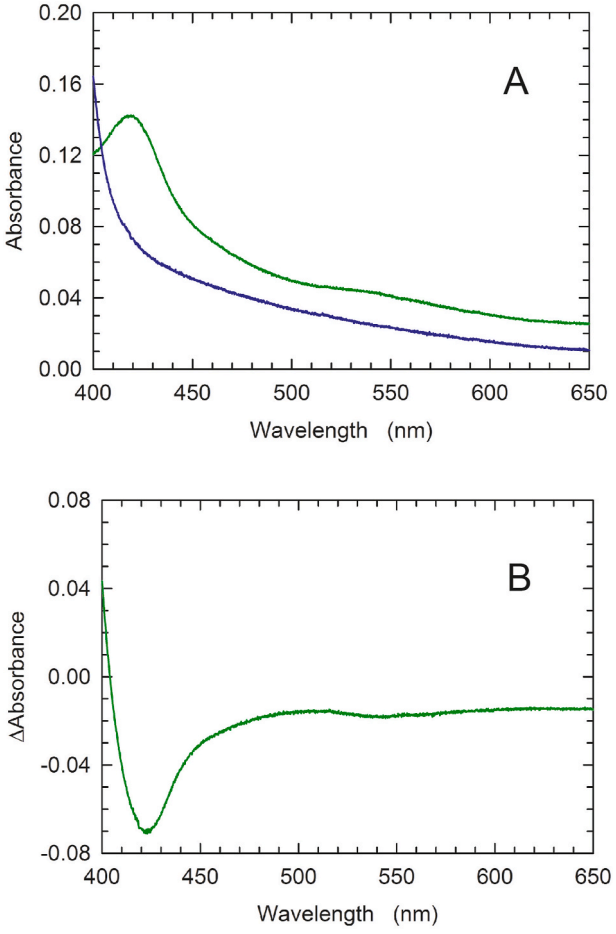

Fig. 6. Absorption spectrum of hDLDH-1 under oxidizing and reducing conditions.
(**A**) The absorption spectrum of 285 μM hDLDH-1 in 10 mM Tris-HCl buffer (pH 7.5, aerobic solution) is reported with a green line. The blue line represents the absorption spectrum of the same protein after addition of an excess of sodium dithionite. (**B**) Reduced minus oxidized difference spectrum obtained with the spectra shown in (A).

Surprisingly enough, when these enzyme solutions were subjected to atomic emission spectroscopy, no iron was detected, neither in hDLDH-1 nor in hDLDH-2. Indeed, we analyzed samples containing 12.2 and 6.5 μM hDLDH-1 and hDLDH-2, respectively, and the analytical limit of detection was determined as equal to 0.4 μM (Supplementary Fig. S4). Taking into account the absence of a heme cofactor and of a FeS cluster in hDLDH, the peculiar spectra of both human D-LDH isoforms (Fig. 5D) could be due to the protein environment inducing an unusual absorption of visible light by FAD, as it was shown for the so-called bifurcating electron transfer flavoproteins [58–60]. Finally, it should be mentioned that the unexpected spectroscopic behaviour of hDLDH-1 and hDLDH-2 could alternatively be interpreted assuming that they contain a flavin derivative such as 6-OH FAD or F_{420}, whose visible absorption spectra do closely resemble those we detected with the human D-lactate isoforms [61,62]. However, it should also be noted that *Escherichia coli* was used to overexpress hDLDH, and that this bacterial host is unable to produce F_{420} [63,64].

3.4. Kinetics of D-lactate oxidation by hDLDH isoforms

As a first test of the catalytic action of hDLDH we assessed the enzyme stereospecificity. To this aim, we assayed the hDLDH-1 activity at the expense of D- and L-lactate. In particular, the assays were performed at pH 7.5 in the presence of 15 mM D- or L-lactate, using 2,6-dichlorophenol indophenol (DCPIP) as electron acceptor. As expected, hDLDH-1 was found strictly stereoselective, being unable of oxidizing L-lactate over a 10 min time interval (Fig. 7A). On the contrary, under the same conditions the enzyme oxidized 6.4 μM D-lactate, with this value obtained converting to concentration the Absorbance decrease observed over 10 min (Fig. 7A). To this aim, the molar extinction coefficient of DCPIP at 600 nm was used (see Methods). Interestingly, the catalytic action of hDLDH-1 was found to be significantly stimulated by the presence in the reaction mixture of 0.1 % (w/v) Triton X-100 (Fig. 7A). Quantitatively speaking, the initial velocity of the reaction was determined as equal to 16.5 ± 0.1 and 26.7 ± 0,2 nM/s in the absence and in the presence of the neutral detergent, respectively (Supplementary Fig. S5). Quite intriguingly, the activity of hDLDH-1 at the expense of D-lactate was found to be completely abolished by the addition of 0.1 % (w/v) SDS to the reaction mixture (Fig. 7A). Therefore, considering the competence of Triton X-100 in enhancing the catalytic action of hDLDH-1 we decided to supplement with this detergent the reaction mixtures used to determine the kinetic parameters of hDLDH-1 and hDLDH-2. By this means, when the activity of hDLDH-1 was assayed as a function of D-lactate concentration in the presence of 50 μM DCPIP, we determined K_m and V_{max} as equal to 0.43 ± 0.04 mM and 31.2 ± 0.5 nM/s, respectively (Fig. 7B). Remarkably, activity assays performed with hDLDH-2 under the same conditions yielded K_m and V_{max} values equal to 0.92 ± 0.11 mM and 20.2 ± 0.6 nM/s, respectively (Fig. 7B). This implies that hDLDH-1 features a catalytic efficiency outperforming that of hDLDH-2, with k_{cat}/K_m values equal to 72 and 22 $M^{-1}s^{-1}$ for hDLDH-1 and hDLDH-2, respectively (Table 1). Considering the relevance of this difference, we carried out an additional experiment, the output of which confirmed the better catalytic performance of hDLDH-1. With an independent series of activity assays performed as a function of D-lactate concentration, we indeed determined for hDLDH-1 and hDLDH-2 K_m values equal to 0.49 ± 0.07 and 0.80 ± 0.07 mM, respectively, with the corresponding V_{max} values estimated as equal to 29.3 ± 0.8 and 16.6 ± 0.3 nM/s (Table 1, Supplementary Fig. S6). This translates into k_{cat}/K_m values equal to 59 and 21 $M^{-1}s^{-1}$ for hDLDH-1 and hDLDH-2, respectively (Table 1). According to its better catalytic efficiency at the expense of D-lactate in the presence of DCPIP as electron acceptor, isoform 1 was selected to further characterize the kinetic properties of hDLDH. In particular, we considered of interest to test the competence of purified hDLDH-1 in transferring electrons to decylubiquinone, as it was previously shown for hDLDH associated to mitochondrial membrane enriched fractions [40]. As a preliminar analysis, we determined the absorption coefficient of the electron acceptor, obtaining a value for decylubiquinone at 275 nm equal to 10000 ± 200 $M^{-1}cm^{-1}$ (Supplementary Fig. S7). Subsequently, by performing activity tests at this wavelength we obtained a K_m value for decylubiquinone equal to 12.5 ± 1.8 μM, with 71.1 ± 2.1 nM/s as the V_{max} determined under these conditions (Fig. 7C). Finally, we assayed hDLDH-1 in the presence of 15 mM D-lactate, using 50 μM cyctochrome *c* as electron acceptor. Surprisingly, no significant reduction of cytochrome *c* was detected, pointing out against any productive interaction of this hemoprotein with hDLDH-1 (Fig. 7D).

3.5. Inhibitors of hDLDH

Considering that the catalytic action of hDLDH could support the energetic metabolism of cancer cells, we thought it might be of interest searching inhibitors of this enzyme.

First, we selected a small set of amino acids whose structural features suggest them as appealing candidates, and we compared the inhibitory action, if any, of both enantiomers of each member of the selected repertoire. Accordingly, activity assays were performed with hDLDH-1, in the absence or in the presence of the amino acid (at 10 mM final concentration) to be tested. In particular, we reasoned that D-alanine could represent a quite promising antagonist of hDLDH. However, contrary to our expectation, this amino acid was ineffective against

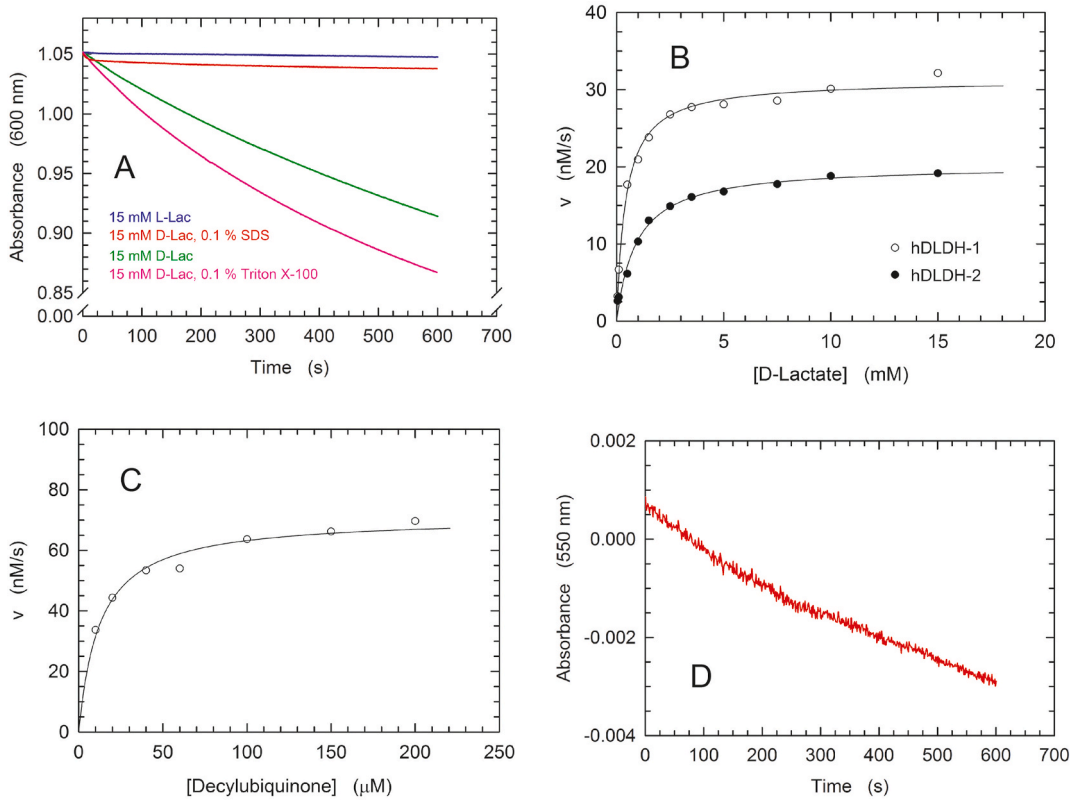

Fig. 7. Catalytic action of human D-lactate dehydrogenase.
(**A**) Kinetics of DCPIP reduction exerted by 1 μM hDLDH-1 at the expense of D-lactate in the absence (green line) or in the presence of surfactants (SDS or Triton X-100, red and magenta lines, respectively). The outcome of an assay performed in the presence of L-lactate (blue line) is also shown. (**B**) Dependence of the initial velocity of DCPIP reduction on D-lactate concentration, determined in the presence of 1 μM of hDLDH-1 (white circles) or hDLDH-2 (black circles), in 50 mM Tris-HCl, 0.1 % (w/v) Triton X-100, pH 7.5, containing 50 μM DCPIP. (**C**) Initial velocity of D-lactate oxidation as a function of decylubiquinone concentration, in the presence of 15 mM D-lactate, 1 μM hDLDH-1 in 50 mM Tris-HCl, pH 7.5. (**D**) Assay of cytochrome *c* reduction by hDLDH-1 performed in the presence of 15 mM D-lactate, 50 μM electron acceptor, and 1 μM enzyme in 50 mM Tris-HCl, pH 7.5.

Table 1
Kinetic parameters of hDLDH-1 and hDLDH-2 determined under steady-state conditions.

Donor	Acceptor	Isoform	V_{max} (nM/s)	k_{cat} (s^{-1})	K_m (mM)
0.05–15 mM D-Lactate	50 μM DCPIP	hDLDH-1	31.2 ± 0.5	0.031	0.43 ± 0.04
0.05–15 mM D-Lactate	50 μM DCPIP	hDLDH-1	29.3 ± 0.8	0.029	0.49 ± 0.07
0.05–15 mM D-Lactate	50 μM DCPIP	hDLDH-2	20.2 ± 0.6	0.020	0.92 ± 0.11
0.05–15 mM D-Lactate	50 μM DCPIP	hDLDH-2	16.6 ± 0.3	0.017	0.80 ± 0.07
15 mM D-Lactate	10–200 μM DecylUQ	hDLDH-1	71.1 ± 2.1	0.071	0.013 ± 0.002

hDLDH-1, and the same was observed for L-alanine (Fig. 8A). Moreover, no significant effect on the target enzyme was triggered by valine and aspartate, independently of the enantiomer considered (Fig. 8A). Notably, we only found a weak, albeit significant, inhibition of hDLDH-1 exerted by D-serine, whereas L-serine proved to be devoid of any inhibitory action (Fig. 8A).

We then assayed the effectiveness of oxalate, oxamate and pyruvate as antagonists of hDLDH-1. Rather surprisingly, oxalate did strongly inhibit D-lactate oxidation, with the corresponding reaction velocity more than halved in the presence of μM concentrations of this dicarboxylic acid (Fig. 8B). Furthermore, oxamate was also found to effectively inhibit hDLDH-1, albeit its action was observed to be weaker when compared to that of oxalate (Fig. 8B). Surprisingly enough, pyruvate was observed to feature a modest competence in inhibiting hDLDH-1, with mM concentrations of this monocarboxylic acid necessary to lower by 20–30 % the enzyme activity (Fig. 8B). Quantitatively speaking, the action of oxalate, oxamate, and pyruvate against hDLDH-1 was inspected according to the equation reported by Burlingham and Widlanski [52] (see Methods), which does linearly relate enzyme activity, inhibitor concentration and K_i. By this means, a biphasic dependence of initial reaction velocity on oxalate concentration was determined, suggesting that hDLDH-1 contains two binding sites for oxalate, featuring high and low affinity, respectively (Fig. 8C). In particular, we obtained for these two binding sites K_i values equal to 1.2 ± 0.3 and 11.3 ± 0.6 μM (Fig. 8C). Interestingly enough, when the same method was used to determine the K_i values for oxamate and pyruvate, a simple linear dependence of initial reaction velocity on inhibitor concentration was observed, with the respective behaviours translating into K_i values equal to 11.1 ± 0.1 and 62.2 ± 2.6 μM (Fig. 8D).

3.6. The catalytic activity exerted by the hDLDH site–specific variants W323C and T412 M

As previously mentioned, it was recently shown that the hDLDH-coding gene of two patients suffering of D-lactate acidosis features a site-specific mutation, i.e. 1122G > T and 1388C > T [46]. This translates into the W323C and the T412 M variants of hDLDH (W374C and T463 M with precursor coordinates, respectively), which are responsible for the increase of D-lactate concentration in plasma to ca. 1100 and 700 μM, respectively, against levels <100 μM detected in wild-type

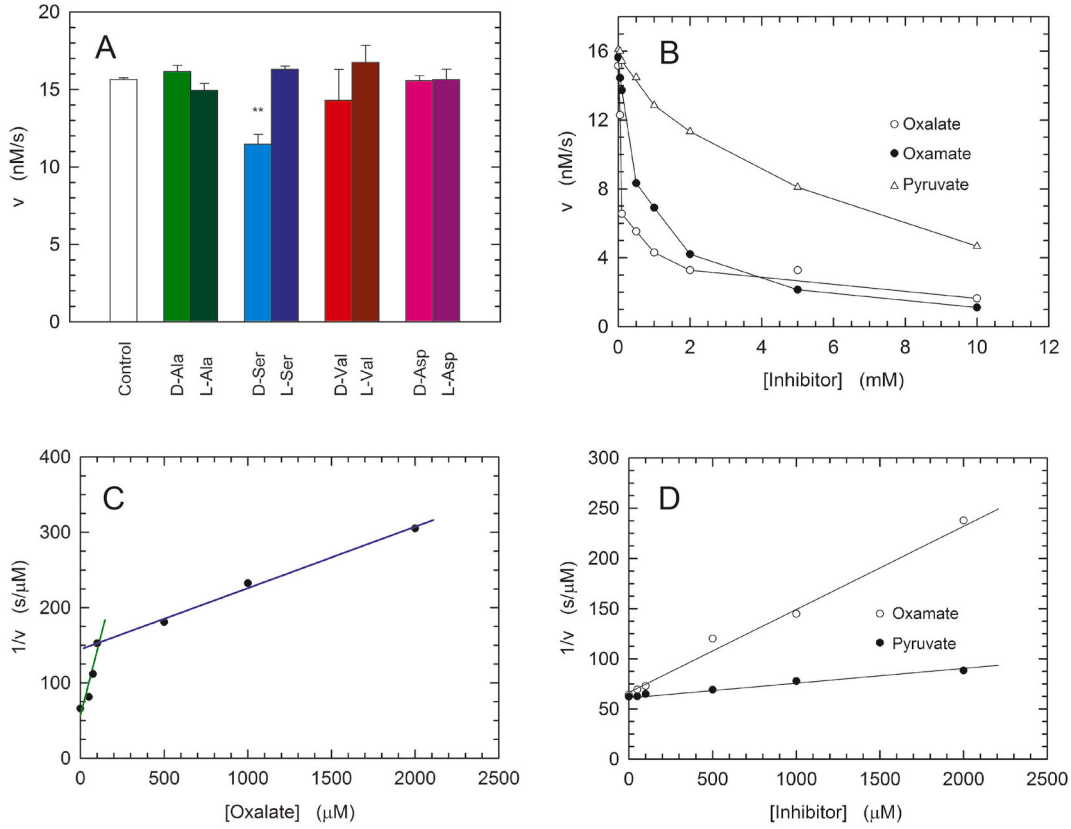

Fig. 8. Inhibition of the catalytic action of hDLDH-1.
(**A**) The activity of hDLDH-1 was tested in the absence (white bar) or in the presence of the indicated L- or D-amino acids. Assay mixtures contained 15 mM D-lactate, 50 µM DCPIP, and 1 µM enzyme in 50 mM Tris HCl, pH 7.5. When present, amino acids were used at 10 mM final concentration. Experimental values were compared by Student's *t*-test (** denotes $P < 0.01$). (**B**)
Inhibitory effect of oxalate, oxamate, or pyruvate against the catalytic action of 1 µM hDLDH-1 exerted in 50 mM Tris-HCl (pH 7.5) at the expense of 15 mM D-lactate in the presence of 50 µM DCPIP, and various inhibitor concentrations. (**C,D**) Analysis of the data reported in Fig. 8B to estimate the value of the K_i of oxalate (**C**), oxamate (**D**) and pyruvate (**D**). A linear equation was used to analyze the experimental observations, with the slopes accordingly determined containing K_i as a free parameter used in the fitting procedure (see Methods).

individuals [46]. To further investigate this interesting point, we constructed both site-specific variants of hDLDH-1, the overexpression and the purification of which were performed with the same procedure used for the wild-type enzyme. Notably, high and similar yields were obtained for the W323C and T412 M mutants (Fig. 9A), and the activity of both variants was tested in the presence of 15 mM D-lactate, with 50 µM DCPIP or 100 µM decylubiquinone as electron acceptor. When the reduction of DCPIP was assayed, the activity of both enzyme variants was found less effective than the catalytic action exerted by the wild-type enzyme (Fig. 9B). Moreover, the W323C mutant of hDLDH-1 was slightly less performant than the T412 M enzyme variant (Fig. 9B). Remarkably, when decylubiquinone was used as electron acceptor, the restraining effect induced by the W323C and T412 M mutations on hDLDH-1 catalytic action was more pronounced than that observed in the presence of DCPIP (Fig. 9C). Quantitatively speaking, the W323C and T412 M mutations do respectively trigger a decrease of the activity down to: i) 39 and 46 % of that detected using wild-type hDLDH-1 and DCPIP as electron acceptor (Fig. 9D); ii) 16 and 32 % of that determined in the presence of wild-type enzyme and decylubiquinone (Fig. 9D). Altogether, these observations are in agreement with those reported by Monroe et al. [46], and represent the first identification, at the protein level, of amino acids engaged in the catalytic action of hDLDH-1. Moreover, it is important to note that the same mutation triggers a major effect on hDLDH-1 when the enzyme activity is assayed in the presence of decylubiquinone instead of DCPIP (Fig. 9D). This, in turn, suggests that W323 and T412 are particularly relevant in the binding of decylubiquinone, with W323 being of primary importance in this event.

4. Discussion

As previously mentioned, human D-lactate dehydrogenase has never been studied at the protein level, and we were accordingly prompted to inspect the structural and functional properties of this enzyme. Structurally speaking, we investigated the secondary and quaternary structure of the two hDLDH isoforms, along with the identity of their cofactor. Concerning the secondary structure of hDLDH-1 and hDLDH-2, we obtained a reasonable agreement of the relative abundance of α-helices, β-strands and coils as determined by CD spectroscopy (Fig. 5) with the corresponding distribution predicted by AlphaFold (Fig. 1). Nevertheless, a different proportion of residues occurring in α-helices and coils was determined by CD spectroscopy and by AlphaFold, with a quite pronounced difference observed for hDLDH-2. To further inspect this point, we analyzed a lactate dehydrogenase the tertiary structure of which was experimentally obtained. In particular, we selected the structure of rabbit lactate dehydrogenase reported by Swiderek et al. [65], to be compared with the model predicted by AlphaFold and with the experimental data we obtained by CD spectroscopy (Supplementary Fig. S8). When the structure obtained by X-ray diffraction is analyzed, the relative abundance of amino acids occurring in α-helices, β-strands and coils equals 50, 22, and 28 %, respectively. These values do respectively translate into 47, 13, and 40 % when the model provided by AlphaFold is taken into account, and into 46, 23, and 31 % when the far UV CD spectrum is used to estimate the elements of rabbit LDH

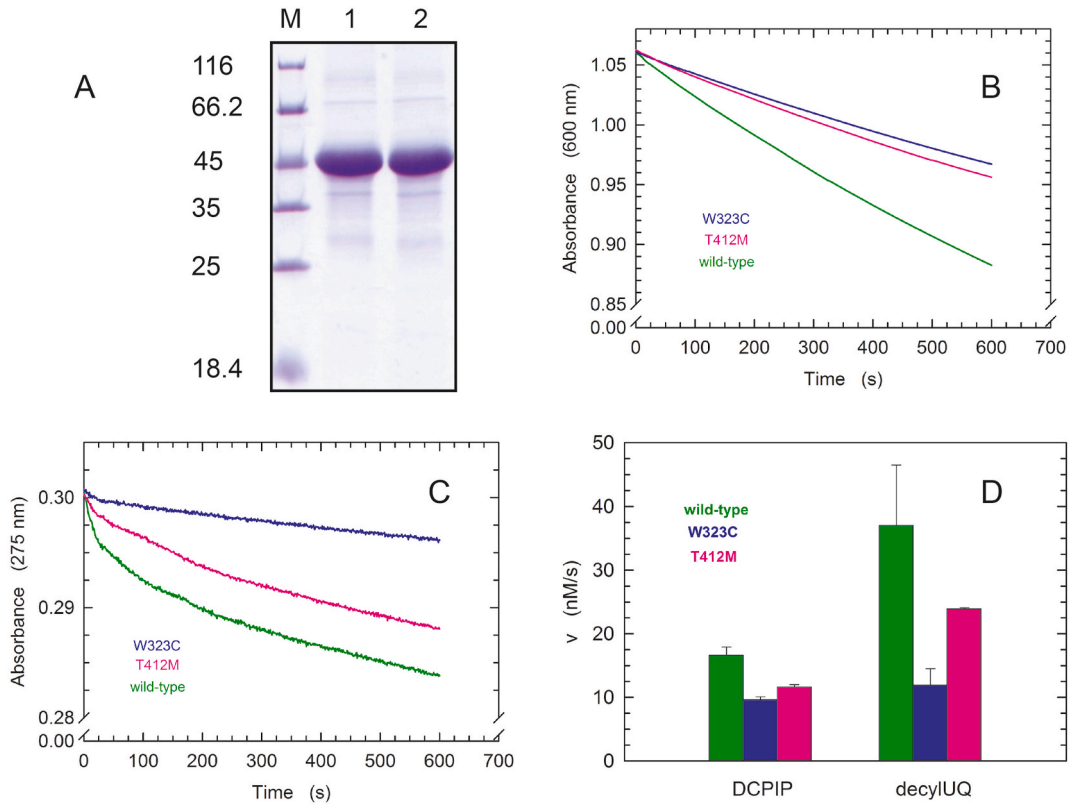

Fig. 9. Catalytic activity of the site-specific variants W323C and T412 M of human D-lactate dehydrogenase.
(**A**) SDS-PAGE of purified T412 M (lane 1) and W323C (lane 2) site-specific variants of human D-lactate dehydrogenase. The molecular masses (kDa) of the loaded markers (lane M) are indicated at the left. (**B**) Kinetics of DCPIP reduction at the expense of D-lactate catalyzed by 1 μM hDLDH-1 wild-type (green line), and by the variants W323C (1.5 μM, blue line), and T412 M (1.5 μM, magenta line). The reaction mixture contained 15 mM D-lactate, 50 μM DCPIP, in 50 mM Tris HCl, pH 7.5. (**C**) Kinetics of decylubiquinone reduction at the expense of D-lactate catalyzed by hDLDH-1 wild-type (1 μM, green line), and by the variants W323C (2 μM, blue line), and T412 M (2 μM, magenta line). Assays were performed in the presence of 15 mM D-lactate, 100 μM decylubiquinone, in 50 mM Tris HCl, pH 7.5. (**D**) The catalytic action at the expense of D-lactate in the presence of the electron acceptor DCPIP (left bars) or decylubiquinone (right bars) is shown for the wild-type, the W323C variant, and the T412 M mutant (green, blue, and magenta bars, respectively). The values of initial reaction velocity (nM/s) were normalized to an enzyme concentration equal to 1 μM per assay. The error bars represent standard deviation. Assay conditions as in Figs 9B and 9C.

secondary structure. Accordingly, it seems unlikely that the approach selected here to interpret the CD spectra of hDLDH (i.e. the use of the K2D algorithm, [54]) is affected by a major shortcoming. On the contrary, the CD spectra of the two hDLDH isoforms (Fig. 5) indicate that these enzymes were appropriately refolded after their solubilization by sarkosyl from inclusion bodies.

Quite intriguingly, the gel filtration and the DLS experiments shown here (Fig.s 2–4) suggest a hexameric and a tetrameric quaternary structure for hDLDH-1 and hDLDH-2, respectively. However, it cannot be ruled out that hDLDH-1 features a tetrameric assembly. This alternative interpretation is sustained by the presence in hDLDH-1 of a considerable loop (containing residues 159–181), the longitudinal extension of which, according to the structural model provided by AlphaFold, is equal to about 2.20 nm (Supplementary Fig. S9). This value corresponds to one third of the extension along the same direction of the whole protein (Supplementary Fig. S9). Accordingly, the overall molecular mass of hDLDH-1 might be overestimated by gel filtration and DLS techniques. It should also be noted that the tetrameric assembly represents a recurrent type of quaternary structure among D-lactate dehydrogenases [11].

According to previous observations obtained with human cell lines, FAD is the cofactor of hDLDH [40]. The presence of a FAD-binding site in hDLDH is also sustained by superimposing the tertiary structure of *Escherichia coli* D-LDH [66] with the structural model of the human D-lactate dehydrogenase generated by AlphaFold. Definitely, these two structures feature a high degree of structural homology (Fig. 10A), which translates into a RMSD value equal to 1.523 Å (605 atoms considered). It is also interesting to note that the primary structures of the *E. coli* and the human enzyme differ considerably, featuring 19.7 % of identity and 31.7 % of similarity (Supplementary Fig. S10), with this poor overlap suggesting a high versatility of AlphaFold in predicting tertiary structures. Remarkably, the structural similarity holds in the region of the *E. coli* enzyme responsible for the binding of FAD (Fig. 10B). Moreover, according to the AlphaFold model of hDLDH the great majority of the hydrogen bonds that the bacterial enzyme engages with FAD [66] are conserved in the human counterpart (Fig. 10C–Table 2). Specifically, among the seven homologous hydrogen bonds, five are characterized by a shorter donor-acceptor distance in the human enzyme, with only one featuring a considerable increased length in hDLDH (Table 2). A similar situation holds when the van der Waals interactions between enzyme and FAD are considered. In particular, it was shown that 6 residues of the *E. coli* enzyme undertake van der Waals interactions with FAD [66]. Remarkably, 4 of these interactions are conserved in the human D-lactate dehydrogenase (Fig. 10D). We therefore propose that the FAD-hDLDH interactions reported here are plausible, suggesting that the construction of site-specific variants of the human enzyme to obtain the apoenzyme represents an interesting point for future studies (see Fig. 11).

Functionally speaking, we have shown here that hDLDH is a strictly stereospecific enzyme, with L-lactate being rejected as substrate (Fig. 7A). In addition to this qualitative feature, we have also demonstrated the opposite action exerted on hDLDH by Triton X-100 and SDS, with the neutral and anionic detergent activating and inhibiting the enzyme, respectively. Interestingly, it was previously reported that

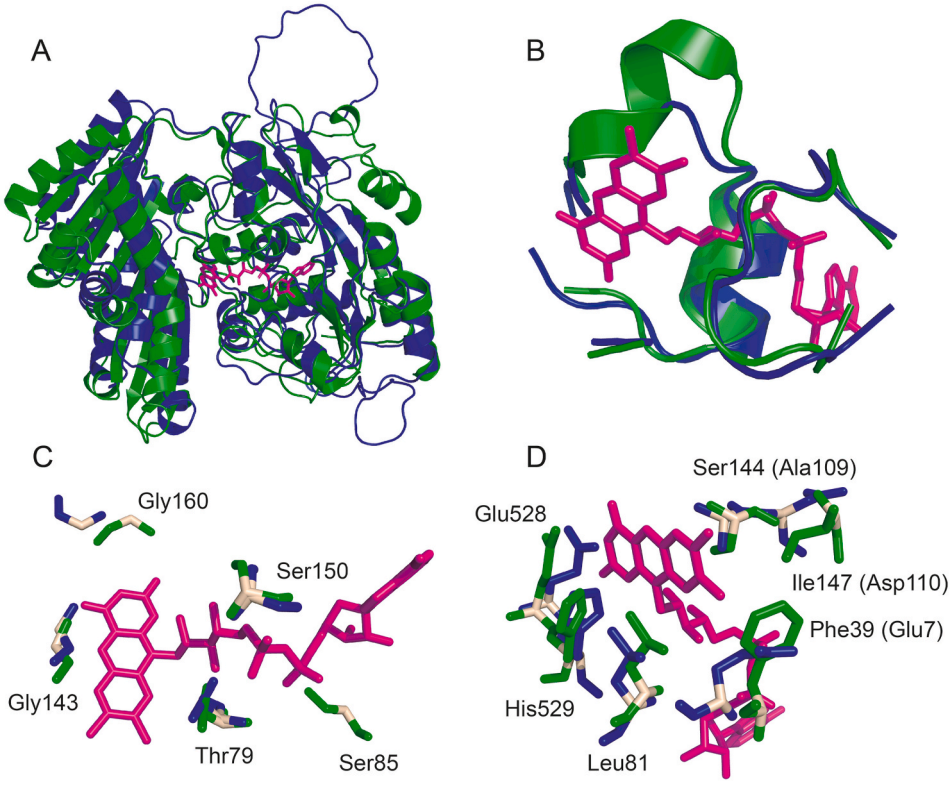

Fig. 10. Structural analysis of the FAD-binding site of human D-lactate dehydrogenase.
(**A**) Structural comparison obtained by superimposing the model of hDLDH molecular architecture (file PDB AF-Q86WU2–F1-model_v4) on the tertiary structure of *Escherichia coli* D-lactate dehydrogenase (file PDB 1F0X). The human and the bacterial enzyme are represented in blue and in green, respectively. The FAD bound to the *E. coli* enzyme is shown with magenta sticks. (**B**) Detail of the FAD-binding site. (**C**) The amino acids of *E. coli* DLDH engaging hydrogen bonds with FAD are shown with green sticks (the α-carbon is represented in salmon). The corresponding amino acids of human D-lactate dehydrogenase are reported with blue sticks. The numberings refer to the residues of the bacterial enzyme. The lengths of the hydrogen bonds are reported in Table 2. (**D**) van der Waals interactions between FAD and *E. coli* DLDH residues (shown with green sticks, α-carbon in salmon). The amino acids of the human D-lactate dehydrogenase residing in analogous positions are reported with blue sticks. The numberings refer to the residues of the bacterial enzyme, and the numbers in brackets indicate amino acids of the human D-lactate dehydrogenase.

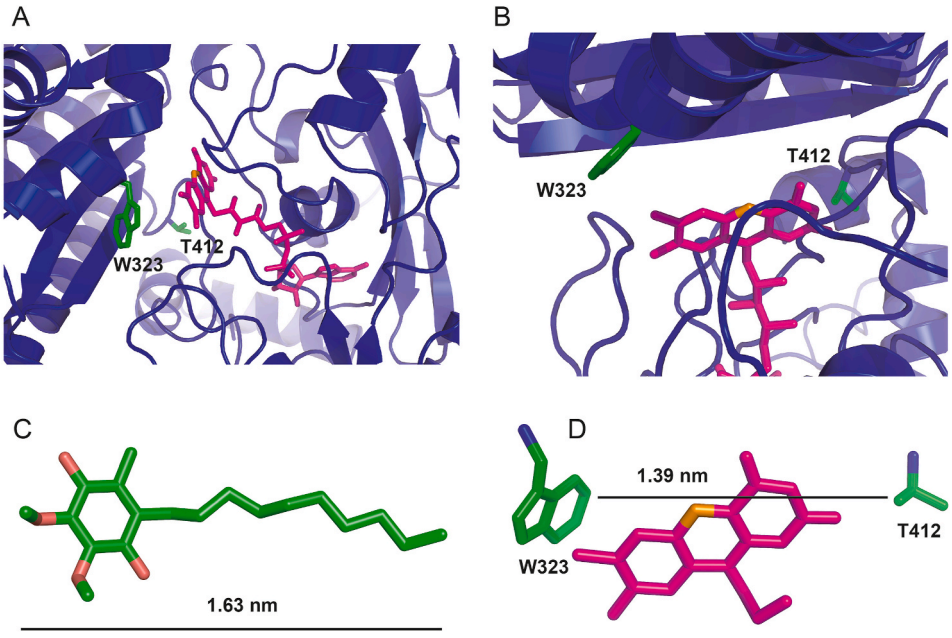

Fig. 11. Location of W323 and T412 in the FAD-binding site of human D-lactate dehydrogenase.
(**A**,**B**) Detail of the FAD-binding region of human D-lactate dehydrogenase. W323 and T412 are shown with green sticks, FAD is represented in magenta with its redox center depicted in orange. (**C**) Structure of decylubiquinone. The black line represents the longitudinal axis of the molecule, the length of which is reported in nm. (**D**) The shortest distance between W323 and T412 of hDLDH is shown with a black line, and its magnitude is indicated in nm.

Table 2
Hydrogen bonds between FAD and amino acids of *Escherichia coli* or human D-lactate dehydrogenase.

FAD	Hydrogen bonds DLDH-FAD			
	Amino acid (*E. coli*)	Distance (Å)	Amino acid (hDLDH)	Distance (Å)
O2P	T79 (O)	2.6	T99 (O)	2.2
O3P	T79 (O)	2.6	T99 (O)	2.0
O2P	T79 (N)	2.9	T99 (N)	2.9
AO5	S85 (O)	2.9	–	–
O4	G143 (N)	3.2	G159 (N)	2.6
O1P	S150 (O)	4.2	S163 (O)	3.7
O1P	S150 (N)	2.8	S163 (N)	2.6
O2	G160 (N)	2.9	G174 (N)	5.1

The indicated distances between FAD and amino acids were determined with PyMol.

Triton X-100 activates the dihydroorotate dehydrogenase from *Plasmodium falciparum*, an enzyme associated to the inner mitochondrial membrane and using ubiquinone as electron acceptor [67]. Moreover, the activation triggered by Triton X-100 was also detected under the following conditions: i) at concentrations of the neutral detergent lower than its CMC; ii) and in the presence of 10 μM ubiquinone-1, i.e. a concentration below the solubility limit in water of this electron acceptor [67]. Accordingly, Triton X-100 appears to assist the binding of the substrate of dihydroorotate dehydrogenase independently of the occurrence of detergent micelles, and we propose that a similar activation is exerted by Triton X-100 on hDLDH. To quantitatively analyze the kinetic parameters of hDLDH, the oxidation of D-lactate was first assayed using 50 μM DCPIP as electron acceptor. Under these conditions, hDLDH-1 was found significantly more efficient than hDLDH-2, featuring a lower K_m for the monocarboxylic acid and a higher V_{max} (Table 1). Concerning the K_m for D-lactate, the mean value equal to 0.46 mM which we obtained using hDLDH-1 (Table 1), is significantly lower than the corresponding value determined for hDLDH with human mitochondrial membrane enriched fractions, i.e. 3 mM [40]. However, it should be also mentioned that the K_m for D-lactate of the *E. coli* purified enzyme sweeps within the 0.3–0.7 mM concentration range [68,69], i.e. between values compatible with the corresponding K_m determination reported here for hDLDH-1. This similarity does not hold when V_{max} is considered: the maximal velocity of the reaction catalyzed by the *E. coli* enzyme was determined as equal to 72–250 μmol/min per mg of protein [68,69], which implies a magnitude (2–7)•10^3 times higher when compared to the corresponding parameter of hDLDH-1, i.e. 30 nM/s in the presence of 1 μM enzyme, which translates into a k_{cat} equal to 0.03 s^{-1} (Table 1). Nevertheless, it should also be mentioned that the k_{cat} values reported for NAD-dependent D-lactate dehydrogenases span a quite large interval, from 0.07 to 910 s^{-1} [70,71]. In particular, the enzyme from *Bacillus coagulans* not only features a k_{cat} (0.07 s^{-1}) the extent of which is similar to that of hDLDH-1, but does also possess a relatively high K_m for D-lactate, i.e. 9.5 mM [70]. Accordingly, when the catalytic efficiency (k_{cat}/K_m) is considered, the human enzyme does largely outperform the *Bacillus coagulans* D-lactate dehydrogenase. Considering that the catalytic action of hDLDH should rely on ubiquinone as the electron acceptor, further activity assays were performed using hDLDH-1 in the presence of 15 mM D-lactate and variable concentrations of decylubiquinone. By this means, the K_m for the electron acceptor was determined as equal to 13 ± 2 μM, and the V_{max} value was estimated as 71 ± 2 nM/s, which translates into a k_{cat} of 0.07 s^{-1} (Table 1). Interestingly, when the activity of *Pseudomonas putida* D-lactate dehydrogenase was assayed as a function of coenzyme Q10 concentration in the presence of 1 mM D-lactate, the K_m for the electron acceptor was determined as 4.1 ± 0.4 μM [72], a value which is of the same order of magnitude of the corresponding kinetic parameter of the human enzyme. Notably, using mitochondrial membrane enriched fractions hDLDH was previously shown to be competent in transferring electrons from D-lactate to cytochrome *c*, with this competence being fully sensitive to Antimycin A [40]. We therefore tested the action of hDLDH-1 at the expense of D-lactate, in the presence of horse heart cytochrome *c* as electron acceptor. Despite we used a relatively high concentration of cyctochrome *c* (50 μM) in this assay, we did not detect its reduction at a significant level (Fig. 7D). This observation is not surprising when considering that hDLDH is topologically associated with the matrix side of the inner mitochondrial membrane, and therefore should be unable to associate with the intermembrane-located cytochrome *c*. Accordingly, the reaction observed with mitochondrial membrane enriched fractions occurs via the bc_1 complex, and is sensitive to Antimycin A.

Taking into account the potential importance of hDLDH in a number of pathological affections, we tested the inhibitory action exerted by different compounds on hDLDH (Fig. 8). Among the DLDHs subjected to a quantitative analysis of their inhibition by mono- or di-carboxylic acids, the NAD-dependent enzymes from *Pseudomonas aeruginosa* and *Lactobacillus pentosus* were studied to evaluate their sensitivity towards pyruvate and oxamate, respectively [13,73]. In addition, the inhibition exerted by oxalate on the NAD-independent DLDH from *Rhodopseudomonas palustris* was investigated [74]. The K_i values accordingly determined are: i) 1.8 ± 0.1 mM for pyruvate against the *P. aeruginosa* enzyme; ii) 2.8 mM for oxamate antagonizing the *L. pentosus* DLDH; iii) 120 μM for the inhibition of oxalate on the *R. palustris* D-lactate dehydrogenase. By comparing these values with those reported here for hDLDH-1, the sensitivity to inhibition of the human enzyme appears particularly high, with the action exerted by oxalate associated to the lowest K_i ever reported, being almost an order of magnitude lower than the K_i value for oxalate against hydroxypyruvate reductase from spinach, which is equal to 7 μM [75].

In addition to the functional data concerning wild-type hDLDH, we have reported that the catalytic activity of hDLDH-1 is significantly counteracted by the site-specific mutations W2323C and T412 M (Fig. 9). Being in agreement with previous findings obtained *in vivo* [46], it is of interest to analyze our observations on these two mutations taking into account the structural model of hDLDH provided by AlphaFold. Indeed, this model predicts that W323 and T412 are located at opposite sides of the FAD-binding pocket of human D-lactate dehydrogenase (Figs 11A and 11B). Furthermore, mutations W323C and T412 M are primarily relevant for the binding of decylubiquinone rather than for the binding of DCPIP, and W323 represents the major determinant for the correct positioning of decylubiquinone in the active site of hDLDH (Fig. 9D). This evidence is sustained by the proximity of W323 to the redox moiety of FAD (Figs 11A and 11B), suggesting that the benzoquinone side of decylubiquinone is oriented towards W323 and that the isoprenyl tail of the electron acceptor points in the direction of T412. In addition, it is interesting to note that the distance between W323 and T412 is of the same order of magnitude of the longitudinal extension of decylubiquinone, i.e. 13.9 and 16.3 Å, respectively (Figs 11C and 11D).

5. Concluding remarks

We have reported here on quite a number of functional and structural features of human D-lactate dehydrogenase. Remarkably, no information at the protein level was previously available on this enzyme. It is also important to note that the procedure we used to overexpress and purify human D-lactate dehydrogenase is a rather straightforward process. Therefore, taking advantage of this and considering the structural features of hDLDH presented here, we hope that our observations will prompt further studies dealing with this appealing enzyme.

Data availability

Data will be made available on request.

Funding

This research did not receive any specific grant from funding agencies in the public, commercial, or not-for-profit sectors.

CRediT authorship contribution statement

Alessandra Stefan: Investigation. **Alberto Mucchi:** Investigation. **Alejandro Hochkoeppler:** Conceptualization, Supervision, Writing – original draft, Writing – review & editing.

Declaration of competing interest

The authors declare that they have no known competing financial interests or personal relationships that could have appeared to influence the work reported in this paper.

Appendix A. Supplementary data

Supplementary data to this article can be found online at https://doi.org/10.1016/j.abb.2024.109932.

References

[1] D. Dennis, N.O. Kaplan, D- and L-lactic acid dehydrogenases in *Lactobacillus plantarum*, J. Biol. Chem. 235 (1960) 810–818.
[2] S. Kaufman, S. Korkes, A. Del Campillo, Biosynthesis of dicarboxylic acids by carbon dioxide fixation. V. Further study of the "malic" enzyme of *Lactobacillus arabinosus*, J. Biol. Chem. 192 (1951) 301–312.
[3] K. Kitahara, A. Obayashi, S. Fukui, Racemase I cell-free racemase, Enzymologia 15 (1953) 259–266.
[4] K. Kitahara, A. Obayashi, DL-forming lactic acid bacteria, J. Gen. Appl. Microbiol. 1 (1955) 237–245.
[5] E.I. Garvie, Bacterial lactate dehydrogenases, Microbiol. Rev. 44 (1980) 106–139.
[6] A. Steinbüchel, H.G. Schlegel, Nad-linked L(+)-lactate dehydrogenase from the strict aerobe *Alcaligenes eutrophus*, Eur. J. Biochem. 130 (1983) 321–328.
[7] K. Arai, T. Ishimitsu, S. Fushinobu, H. Uchikoba, H. Matsuzawa, H. Taguchi, Active and inactive state structures of unliganded *Lactobacillus casei* allosteric L-lactate dehydrogenase, Proteins 78 (2009) 681–694.
[8] S. Kochnar, P.E. Hunziker, P. Leong-Morgenthaler, H. Hottinger, Primary structure, physicochemical properties, and chemical modification of the NAD^+-dependent D-lactate dehydrogenase, J. Biol. Chem. 267 (1992) 8499–8513.
[9] A. Razeto, S. Kochnar, H. Hottinger, M. Dauter, K.S. Wilson, V.S. Lamzin, Domain closure, substrate specificity and catalysis of D-lactate dehydrogenase from *Lactobacillus bulgaricus*, J. Mol. Biol. 318 (2002) 109–119.
[10] S. Kim, S. Gu, Y.H. Kim, K. Kim, Crystal structure and thermodynamic properties of D-lactate dehydrogenase from *Lactobacillus jensenii*, Int. J. Biol. Macromol. 68 (2014) 151–157.
[11] B. Jia, Z.J. Pu, K. Tang, X. Jia, K.H. Kim, X. Liu, C.O. Jeon, Catalytic, computational, and evolutionary analysis of the D-lactate dehydrogenases responsible for D-lactic acid production in lactic acid bacteria, J. Agric. Food Chem. 66 (2018) 8371–8381.
[12] G. Le Bras, J. Garel, Properties of D-lactate dehydrogenase from *Lactobacillus bulgaricus*: a possible different evolutionary origin for the D- and L-lactate dehydrogenases, FEMS Microbiol. Lett. 79 (1991) 89–94.
[13] N. Furukawa, A. Miyanaga, M. Togawa, M. Nakajima, H. Taguchi, Diverse allosteric and catalytic functions of tetrameric D-lactate dehydrogenases from the Gram-negative bacteria, Amb. Express 4 (2014) 76.
[14] Y. Takenaka, G.W. Schwert, Lactic dehydrogenase: III. Mechanism of the reaction, J. Biol. Chem. 223 (1956) 157–170.
[15] N.O. Kaplan, M.M. Ciotti, F.E. Stolzenbach, Reaction of pyridine nucleotide analogues with dehydrogenases, J. Biol. Chem. 221 (1956) 833–844.
[16] N.O. Kaplan, M.M. Ciotti, M. Hamolsky, R.E. Bieber, Molecular heterogeneity and evolution of enzymes, Science 131 (1960) 392–397.
[17] G.L. Long, N.O. Kaplan, D-lactate specific pyridine nucleotide lactate dehydrogenase in animals, Science 162 (1968) 685–686.
[18] M.J. Flick, S.F. Konieczny, Identification of putative mammalian D-lactate dehydrogenase enzymes, Biochem. Biophys. Res. Commun. 295 (2002) 910–916.
[19] M.W. Fraaije, W.J.H. van Berkel, J.A.E. Benen, J. Visser, A. Mattevi, A novel oxidoreductase family sharing a consereved FAD-binding domain, Trends Biochem. Sci. 23 (1998) 206–207.
[20] T.A. Ewing, M.W. Fraaije, A. Mattevi, W.J.H. van Berkel, The VAO/PCMH flavoprotein family, Arch. Biochem. Biophys. 632 (2017) 104–117.
[21] D.H. Williamson, P. Lund, H.A. Krebs, The redox state of free nicotinamide-adenine dinucleotide in the cytoplasm and mitochondria of rat liver, Biochem. J. 103 (1967) 514–527.
[22] R. Cammack, Assay, purification and properties of mammalian D-2-hydroxy acid dehydrogenase, Biochem. J. 115 (1969) 55–64.
[23] C.J. Valvona, H.L. Fillmore, P.B. Nunn, G.J. Pilkington, The regulation and function of lactate dehydrogenase A: therapeutic potential in brain tumor, Brain Pathol. 26 (2016) 3–17.
[24] M.R. Woodford, V.Z. Chen, S.J. Backe, G. Bratslavsky, M. Mollapour, Structural and functional regulation of lactate dehydrogenase-A in cancer, Future Med. Chem. 12 (2020) 439–455.
[25] J.A. Read, V.J. Winter, C.M. Eszes, R.B. Sessions, R.L. Brady, Structural basis for altered activity of M- and H-isozyme forms of human lactate dehydrogenase, Proteins 43 (2001) 175–185.
[26] T. Evrev, S. Zhivcov, L. Russev, LDH isozymes in testicular cultures and human testes, Hum. Hered. 20 (1970) 70–73.
[27] K.M. LeVan, E. Goldberg, Properties of human testis-specific lactate dehydrogenase expressed from *Escherichia coli*, Biochem. J. 273 (1991) 587–592.
[28] K. Sahlin, R.C. Harris, B. Nylind, E. Hultman, Lactate content and pH in muscle samples obtained after dynamic exercise, Pflugers Arch. 367 (1976) 143–149.
[29] A. Schurr, R.S. Payne, Lactate, not pyruvate, is neuronal aerobic glycolysis end product: an *in vitro* electrophysiological study, Neuroscience 147 (2007) 613–619.
[30] G.A. Brooks, Lactate: glycolytic end product and oxidative substrate during sustained exercise in mammals – the 'lactate shuttle, in: R. Gilles (Ed.), Circulation, Respiration, and Metabolism: Current Comparative Approaches, Springer Verlag, Berlin, 1985, pp. 208–218.
[31] M.J. Rogatzki, B.S. Ferguson, M.L. Goodwin, L.B. Gladden, Lactate is always the end product of glycolysis, Front. Neurosci. 9 (2015) 22.
[32] J.F. Zilva, The origin of the acidosis in hyperlactatemia, Ann. Clin. Chem. 15 (1978) 40–43.
[33] C. Granchi, S. Bertini, M. Macchia, F. Minutolo, Inhibitors of lactate dehydrogenase isoforms and their therapeutic potentials, Curr. Med. Chem. 17 (2010) 672–697.
[34] R. Rani, V. Kumar, Recent update on human lactate dehydrogenase enzyme 5 (*h*LDH5) inhibitors: a promising approach for cancer chemotherapy, J. Med. Chem. 59 (2016) 487–496.
[35] S. Ray, M. Ray, Isolation of methylglyoxal synthase from goat liver, J. Biol. Chem. 256 (1981) 6230–6234.
[36] D.L. Pompliano, A. Peyman, J.R. Knowles, Stabilization of a reaction intermediate as a catalytic device: definition of the functional role of the flexible loop in triosephosphate isomerase, Biochemistry 29 (1990) 3186–3194.
[37] J.P. Richard, Kinetic parameters for the elimination reaction catalyzed by triosephosphate isomerase and an estimation of the reaction's physiological significance, Biochemistry 30 (1991) 4581–4585.
[38] B. Mannervik, Molecular enzymology of the glyoxalase system, Drug Metabol. Drug Interact. 23 (2008) 13–27.
[39] D. Choi, J. Kim, S. Ha, K. Kwon, E. Kim, H. Lee, K. Ryu, C. Park, Stereospecific mechanism of DJ-1 glyoxalases inferred from their hemithioacetal-containing crystal structures, FEBS J. 281 (2014) 5447–5462.
[40] L. De Bari, L. Moro, S. Passarella, Prostate cancer cells metabolize D-lactate inside mitochondria via a D-lactate dehydrogenase which is more active and highly expressed than in normal cells, FEBS Lett. 587 (2013) 467–473.
[41] S.M. Smith, R.H. Eng, F. Buccini, Use of D-lactic acid measurements in the diagnosis of bacterial infections, J. Infect. Dis. 154 (1986) 658–664.
[42] Y. Kondoh, M. Kawase, Y. Kawakami, S. Ohmori, Concentrations of D-lactate and its related metabolic intermediates in liver, blood, and muscle of diabetic and starved rats, Res. Exp. Med. 192 (1992) 407–414.
[43] F. Caglayan, M. Cakmak, O. Caglayan, T. Cavusoglu, Plasma D-lactate levels in diagnosis of appendicitis, J. Invest. Surg. 16 (2003) 233–237.
[44] M. Pohanka, D-lactic acid as a metabolite: toxicology, diagnosis, and detection, BioMed Res. Int. 2020 (2020) 3419034.
[45] J. Cai, H. Chen, M. Weng, S. Jiang, J. Gao, Diagnostic and clinical significance of serum levels of D-lactate and diamine oxidase in patients with Crohn's disease, Gastroenterol. Res. Pract. 2019 (2019) 8536952.
[46] G.R. Monroe, A.M. van Eerde, F. Tessadori, K.J. Duran, S.M.C. Savelberg, J.C. van Alfen, P.A. Terhal, S.N. van der Crabben, K.D. Lichtenbelt, S.A. Fuchs, J. Gerrits, M. J. van Roosmalen, K.L. van Gassen, M. van Aalderen, B.G. Koot, M. Oostendorp, M. Duran, G. Visser, T.J. de Koning, F. Calì, P. Bosco, K. Geleijns, M.G.M. de Sain-van der Velden, N.V. Knoers, J. Bakkers, N.M. Verhoeven-Duif, G. van Haaften, J. J. Jans, Identification of human D lactate dehydrogenase deficiency, Nat. Commun. 10 (2019) 1477.
[47] L. Scutteri, G. Maltoni, A. Hochkoeppler, Amberlite XAD-4 is a convenient tool for removing Triton X-100 and Sarkosyl from protein solutions, Biotechniques 74 (2023) 45–50.
[48] G. Maltoni, L. Scutteri, F. Mensitieri, F. Dal Piaz, A. Hochkoeppler, High-yield production in *Escherichia coli* and convenient purification of a candidate vaccine against SARS-CoV-2, Biotechnol. Lett. 44 (2022) 1313–1322.
[49] M.M. Bradford, A rapid and sensitive method for the quantitation of microgram quantities of protein utilizing the principle of protein-dye binding, Anal. Biochem. 72 (1976) 248–254.
[50] J.McD. Armstrong, The molar extinction coefficient of 2,6-dichlorophenol indophenol, Biochim. Biophys. Acta 86 (1964) 194–197.
[51] B.F. van Gelder, E.C. Slater, The extinction coefficient of cytochrome *c*, Biochim, Biophys Acta 58 (1962) 593–595.
[52] B.T. Burlingham, T.S. Widlanski, An intuitive look at the relationship of K_i and IC_{50}: a more general use of the Dixon plot, J Chem. Educ. 80 (2003) 214–218.
[53] W.L. DeLano, Use of PyMol as a communication tool for molecular science, Abstr. Pap. An. Chem. Soc. 228 (2004) U313–U314.
[54] M.A. Andrade, P. Chacón, J.J. Merelo, F. Morán, Evaluation of secondary structure of proteins from UV circular dichroism spectra using an unsupervised learning neural network, Protein Eng. 6 (1993) 383–390.

[55] A.J. Miles, S.G. Ramalli, B.A. Wallace, DichroWeb, a website for calculating protein secondary structure from circular dichroism spectroscopic data, Protein Sci. 31 (2021) 37–46.
[56] K. Saeki, K. Tokuda, K. Fukuyama, H. Matsubara, K. Nadanami, M. Go, S. Itoih, Site-specific mutagenesis of *Rhodobacter capsulatus* Ferredoxin I, FdxN, that functions in nitrogen fixation, J. Biol. Chem. 271 (1996) 31399–31406.
[57] S.G. Mayhew, D. Petering, G. Palmer, G.P. Foust, Spectrophotometric titration of ferredoxins and *Chromatium* high potential iron protein with sodium dithionite, J. Biol. Chem. 244 (1969) 2830–2834.
[58] N. Mohamed-Raseek, H.D. Duan, P. Hildebrandt, M.A. Mroginski, A. Miller, Spectroscopic, thermodynamic and computational evidence of the locations of the FADs in the nitrogen fixation-associated electron transfer flavoprotein, Chem. Sci. 10 (2019) 7762–7772.
[59] N.P. Chowdhury, A.M. Mowafy, J.K. Demmer, V. Upadhyay, S. Koelzer, E. Jayamani, J. Kahnt, M. Hornung, U. Demmer, U. Ermler, W. Buckel, Studies on the mechanism of electron bifurcation catalyzed by electron transferring flavoprotein (Etf) and butyryl-CoA dehydrogenase (Bcd) of *Acidaminococcus fermentans*, J. Biol. Chem. 289 (2014) 5145–5157.
[60] K. Sato, Y. Nishina, K. Shiga, Purification of electron-transferring flavoprotein from *Megasphaera elsdenii* and binding of additional FAD with an unusual absorption spectrum, J. Biochem. 134 (2003) 719–729.
[61] C.D. Whitfield, S.G. Mayhew, Evidence that apo-reduced nicotinamide adenine dinucleotide dehydrogenase and apo-electron-transferring flavoprotein from *Peptostreptococcus elsdenii* are identical, J. Biol. Chem. 249 (1974) 2811–2815.
[62] R. Grinter, C. Greening, Cofactor F_{420}: an expanded view of its distribution, biosynthesis and roles in bacteria and archaea, FEMS Microbiol. Rev. 45 (2021) 1–46.
[63] G. Bashiri, J. Antoney, E.N.M. Jirgis, M.V. Shah, B. Ney, J. Copp, S.M. Stuteley, S. Sreebhavan, B. Palmer, M. Middleditch, N. Tokuriki, C. Greening, C. Scott, E. N. Baker, C.J. Jackson, A revised biosynthetic pathway for the cofactor F_{420} in prokaryotes, Nat. Commun. 10 (2019) 1558.
[64] M.V. Shah, H. Nazem-Bokaee, J. Antoney, S.W. Kang, C.J. Jackson, C. Scott, Improved production of the non-native cofactor F_{420} in *Escherichia coli*, Sci. Rep. 11 (2021) 21774.
[65] K. Swiderek, A. Panczakiewicz, A. Bujacz, G. Bujacz, P. Paneth, Modeling of isotope effects on binding oxamate to lactic dehydrogenase, J. Phys. Chem. B 113 (2009) 12782–12789.
[66] O. Dim, E.A. Pratt, C. Ho, D. Eisenberg, The crystal structure of D-lactate dehydrogenase, a peripheral membrane respiratory enzyme, Proc. Natl. Acad. Sci. USA 97 (2000) 9413–9418.
[67] N.A. Malmquist, J. Baldwin, M.A. Phillips, Detergent-dependent kinetics of truncated *Plasmodium falciparum* dihydroorotate dehydrogenase, J. Biol. Chem. 282 (2007) 12678–12686.
[68] Y. Tanaka, Y. Anraku, M. Futai, *Escherichia coli* membrane D-lactate dehydrogenase. Isolation of the enzyme in aggregated form and its activation by Triton X-100 and phospholipids, J. Biochem. 80 (1976) 821–830.
[69] E.A. Pratt, L.W. Fung, J.A. Flowers, C. Ho, Membrane-bound D-lactate dehydrogenase from *Escherichia coli*: purification and properties, Biochemistry 18 (1979) 312–316.
[70] L. Wang, Y. Cai, L. Zhu, H. Guo, B. Yu, Major role of NAD-dependent lactate dehydrogenases in the production of L-lactic acid with high optical purity by the thermophile *Bacillus coagulans*, Appl. Environ. Microbiol. 80 (2014) 7134–7141.
[71] B. Jia, Z.J. Pu, K. Tang, X. Jia, K.H. Kim, X. Liu, C.O. Jeon, Catalytic, computational, and evolutionary analysis of the D-lactate dehydrogenases responsible for D-lactic acid production in lactic acid bacteria, J. Agric. Food Chem. 66 (2018) 8371–8381.
[72] T. Jiang, X. Guo, J. Yan, Y. Zhang, Y. Wang, M. Zhang, B. Sheng, C. Ma, P. Xu, C. Gao, A bacterial multidomain NAD-independent D-lactate dehydrogenase utilizes flavin adenine dinucleotide and Fe-S clusters as cofactors and quinone as an electron acceptor for D-lactate oxidization, J. Bacteriol. 199 (2017) e00342-17.
[73] T. Shinoda, K. Arai, M. Shigematsu-Iida, Y. Ishikura, S. Tanaka, T. Yamada, M. S. Kimber, E.F. Pai, S. Fushinobu, H. Taguchi, Distinct conformation functions of an active site loop in the catalytic reactions of NAD-dependent D-lactate dehydrogenase and formate dehydrogenase, J. Biol. Chem. 280 (2005) 17068–17075.
[74] S. Horikiri, Y. Aizawa, T. Kai, S. Amachi, H. Shinoyama, T. Fujii, Electron acquisition system constructed from an NAD-independent D-lactate dehydrogenase and cytochrome c_2 in *Rhodopseudomonas palustris* No. 7, Biosci. Biotechnol. Biochem. 68 (2004) 516–522.
[75] L.A. Kleczkowski, D.D. Randall, G.E. Edwards, Oxalate as a potent and selective inhibitor of spinach (*Spinacia oleracea*) leaf NADPH-dependent hydroxypyruvate reductase, Biochem. J. 276 (1991) 125–127.